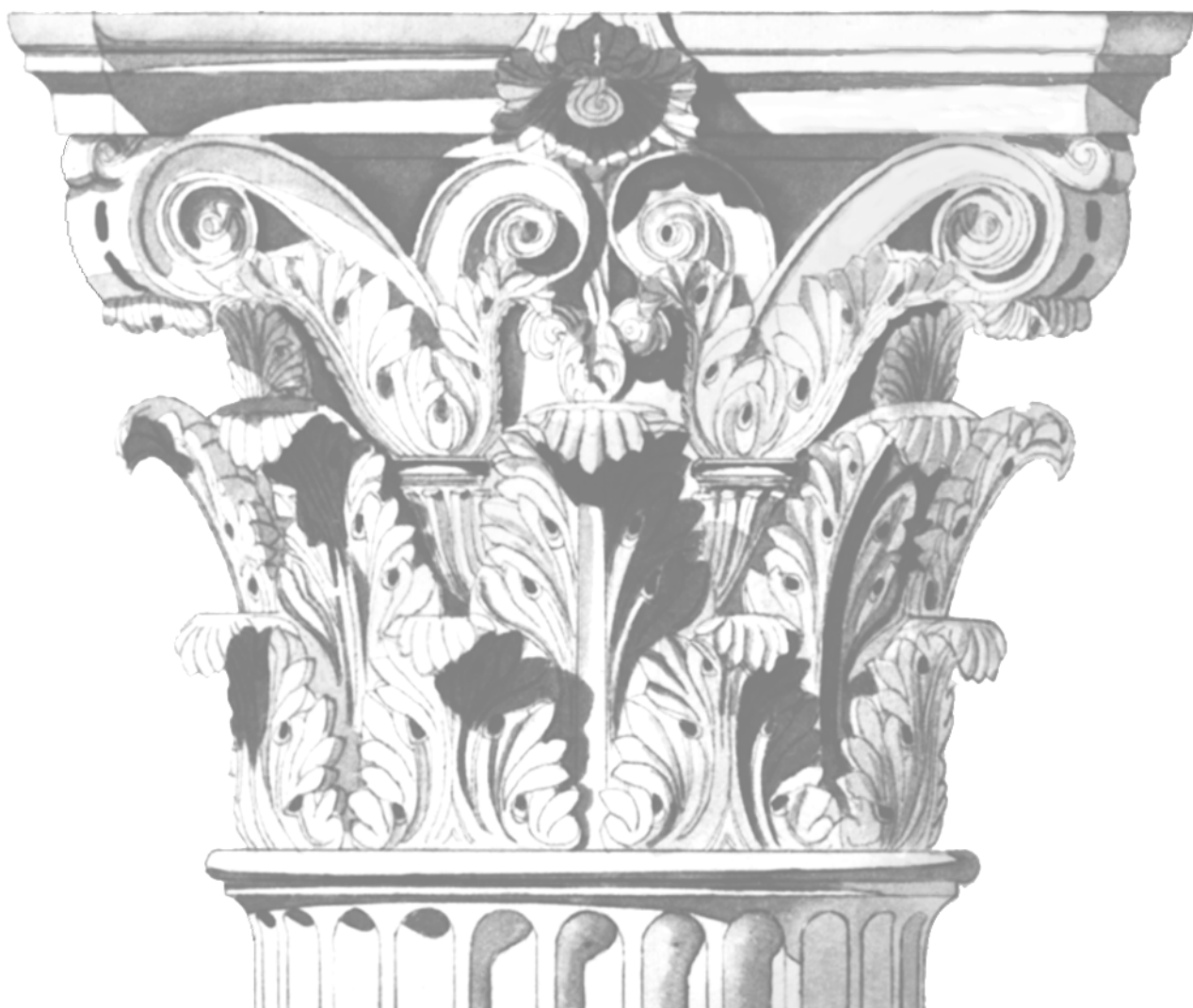


**SUBSTITUENT GROUPS IN
ARYL- AND
ARYLALKYLPHOSPHANES:
EFFECTS ON COORDINATION
CHEMISTRY AND CATALYTIC
PROPERTIES**

**HELENA
RIIHIMÄKI**

Department of Chemistry,
University of Oulu

OULU 2003



HELENA RIIHIMÄKI

**SUBSTITUENT GROUPS IN ARYL-
AND ARYLALKYLPHOSPHANES:
EFFECTS ON COORDINATION
CHEMISTRY AND CATALYTIC
PROPERTIES**

Academic Dissertation to be presented with the assent of the Faculty of Science, University of Oulu, for public discussion in Raahensali (Auditorium L10), Linnanmaa, on June 14th, 2003, at 12 noon.

OULUN YLIOPISTO, OULU 2003

Copyright © 2003
University of Oulu, 2003

Reviewed by
Professor Reija Jokela
Professor Erkki Kolehmainen

ISBN 951-42-7045-2 (URL: <http://herkules.oulu.fi/isbn9514270452/>)

ALSO AVAILABLE IN PRINTED FORMAT

Acta Univ. Oul. A 402, 2003

ISBN 951-42-7044-4

ISSN 0355-3191 (URL: <http://herkules.oulu.fi/issn03553191/>)

OULU UNIVERSITY PRESS

OULU 2003

Riihimäki, Helena, Substituent groups in aryl- and arylalkylphosphanes: effects on coordination chemistry and catalytic properties

Department of Chemistry, University of Oulu, P.O.Box 3000, FIN-90014 University of Oulu, Finland
Oulu, Finland
2003

Abstract

Thirty phosphane ligands were prepared and characterized. Aryl groups of the phosphane ligands were modified through change in functionality. The side chains were the following: trifluoromethylphenyl, selenomethylphenyl, 9-anthryl, alkyl-substituted aryl groups, and pyridyl and alkyl groups. In addition, three chromium carbonyl complexes of potentially bidentate arylphosphanes containing nitrogen heteroatoms were prepared and characterized. Characterization of the isolated complexes verified the monodentate coordination from phosphorus and two bidentate coordination modes, (P,N)-bound and (N,N')-bound.

Ligands and complexes were characterized by ^1H , $^{13}\text{C}\{^1\text{H}\}$, $^{31}\text{P}\{^1\text{H}\}$, and two-dimensional NMR spectroscopy, X-ray crystallography, and mass spectrometry. The $^{13}\text{C}\{^1\text{H}\}$ and $^{31}\text{P}\{^1\text{H}\}$ NMR spectra, and calculated cone angles of the *o*-alkyl-substituted aryl- and arylalkylphosphane ligands provided valuable parameters, which could be plotted against catalytic results in the search for correlations between the structures and catalytic behavior of ligands. Correlations were found between the parameters and the catalytic behavior of Rh-catalysts modified with the *o*-alkyl-substituted phenylphosphanes.

The research reported here was directed toward the preparation and characterization of phosphane ligands which would favor the formation of isobutanal in propene hydroformylation. The *o*-alkyl-substituted arylphosphanes, which were studied most thoroughly, gave the highest selectivity to isobutanal but at the cost of activity. Linear *n*-butanal was still the main product, though only barely. Alkyl substituents in meta position increased the activity of propene hydroformylation even up to the level with the reference ligand PPh_3 , but, the selectivity decreased simultaneously.

Keywords: NMR spectroscopy, *o*-alkyl-substituted arylphosphanes, olefin hydroformylation, preparation

Acknowledgments

The present study was carried out in the Department of Chemistry at the University of Oulu during the years 1999-2003.

I am most grateful to my supervisor Professor Jouni Pursiainen for his guidance and the opportunity he provided to work in the developing field of phosphane ligands. The time and effort he invested during the final hectic months needed to complete the thesis are indeed appreciated. I am indebted to two referees, Professor Erkki Kolehmainen and Professor Reija Jokela, for their thorough reading of the manuscript, and to Dr. Kathleen Ahonen for carefully revising the language.

I wish to thank the "Synco" project team for excellent cooperation and my co-authors for their contributions. Especially, I appreciate the essential advice received from Dr. Riitta Laitinen at the beginning of my work and the helpful and encouraging team-work with Dr. Heidi Reinius, Dr. Pekka Suomalainen, Docent Matti Haukka, Docent Sirpa Jääskeläinen, Teija Kangas, Johanna Suutari, and Merja Harteva. I express my thanks as well to Professor Outi Krause, Professor Tapani Pakkanen, and Dr. Esko Karvinen. Their broad knowledge and advice show through in many parts of my work.

I would like to sincerely thank all my friends and colleagues in the Laboratory of Physical Chemistry, and the staff in the Department of Chemistry for a warm and pleasant working atmosphere. In particular, thanks are extended to Päivi Joensuu and Sari Ek for performing the mass spectra measurements. Special thanks are owed as well to my office mates Leeni and Ari for the conversations we shared, both creative and hilarious.

My parents, Kyllikki and Erkki, provided continuing encouragement and support, while my sisters, their families, and many friends lightened the work with diversions of different kinds. I am deeply appreciative of your contributions. Finally, my warmest thanks to Aslak for inspiring companionship, support, and love.

The study was funded by Neste Oxo AB, the Technology Development Center of Finland and the Inorganic Materials Chemistry Graduate Program, with additional support provided by the Tauno Tönning Foundation, the Finnish Konkordia Foundation, the Emil Aaltonen Foundation, the Alfred Kordelin Foundation, and the Cultural Foundation of Keski-Pohjanmaa.

Oulu, May 2003

Helena Riihimäki

List of original papers

This thesis is based on the following papers, which are referred to in the text by their Roman numerals:

- I Suomalainen P, Reinius HK, Riihimäki H, Laitinen RH, Jääskeläinen S, Haukka M, Pursiainen JT, Pakkanen TA & Krause AOI (2001) Hydroformylation of 1-hexene and propene with in situ formed rhodium phosphine catalysts. *J Mol Catal A: Chem* 169: 67-78.
- II Suomalainen P, Riihimäki H, Jääskeläinen S, Haukka M, Pursiainen JT & Pakkanen TA (2001) Structural and catalytic properties of alkyl-substituted phosphanes. Effect of *ortho*-modification on rhodium-catalyzed 1-hexene hydroformylation. *Catal Lett* 77: 125-130.
- III Reinius HK, Suomalainen P, Riihimäki H, Karvinen E, Pursiainen JT & Krause AOI (2001) *o*-Alkyl-substituted triphenylphosphines: activity and regioselectivity in rhodium-catalysed propene hydroformylation. *J Catal* 199: 302-308.
- IV Riihimäki H, Suomalainen P, Reinius HK, Suutari J, Jääskeläinen S, Krause AOI, Pakkanen TA & Pursiainen JT (2003) *o*-Alkyl-substituted aromatic phosphanes for hydroformylation studies: synthesis, spectroscopic characterization and ab initio investigations. *J Mol Catal A: Chem* 200: 69-79.
- V Riihimäki H, Kangas T, Suomalainen P, Reinius HK, Jääskeläinen S, Haukka M, Krause AOI, Pakkanen TA & Pursiainen JT (2003) Synthesis of new *o*-alkyl-substituted arylalkylphosphanes: study of their molecular structure and influence on rhodium-catalyzed propene and 1-hexene hydroformylation. *J Mol Catal A: Chem* 200: 81-94.

Symbols and abbreviations

acac	acetyl acetate
Bu	butyl
COLOC	correlation spectroscopy via long-range coupling
COSY	correlation spectroscopy
Cy	cyclohexyl
Et	ethyl
HETCOR	heteronuclear correlation
HSQC	heteronuclear single-quantum correlation
i/n	ratio of branched to linear aldehydes
<i>i</i> -Pr	isopropyl
L	ligand
L/Rh	ratio of ligand to rhodium
Me	methyl
MMA	methyl methacrylate
NMe ₂	dimethylamino
NMR	nuclear magnetic resonance
OMe	methoxy
Ph	phenyl
PVC	polyvinylchloride
SMe	thiomethyl
SeMe	selenomethyl
TMEDA	<i>N,N,N',N'</i> -tetramethylethylenediamine
tolyl	methylphenyl

Contents

Abstract	
Acknowledgments	
List of original papers	
Symbols and abbreviations	
1 Introduction	13
1.1 Phosphane ligands	14
1.2 Hydroformylation	15
2 Aims of the work	17
3 Synthetic work	19
3.1 Reagents	19
3.2 General procedure for preparation of phosphanes	19
3.2.1 Trifluoromethyl- and selenomethyl-substituted phenylphosphanes	20
3.2.2 (9-Anthryl)phenylphosphanes	22
3.2.3 Alkyl-substituted arylphosphanes	22
3.2.4 Alkyl-substituted pyridylphosphanes	25
3.2.5 <i>o</i> -Alkyl-substituted arylalkylphosphanes	26
3.3 Cr carbonyl derivatives of phosphane ligands containing nitrogen	27
4 Characterization	29
4.1 Instrumentation and measurements	29
4.2 Structure of phosphane ligands	30
4.2.1 $^{31}\text{P}\{^1\text{H}\}$ NMR spectra and cone angles	30
4.2.2 ^1H and $^{13}\text{C}\{^1\text{H}\}$ NMR spectra	32
4.2.2.1 <i>o</i> -Substituted arylphosphanes	32
4.2.2.2 <i>m</i> -Isopropyl-substituted phenylphosphanes	34
4.2.2.3 Isopropyl and cyclohexyl groups directly bonded to phosphorus	36
4.2.3 X-ray crystal structures	38
4.3 Structure of Cr carbonyl derivatives	39
4.3.1 NMR spectra	40
4.3.2 X-ray crystal structures	42

5 Hydroformylation	44
5.1 Trifluoromethyl- and selenomethyl-substituted phenylphosphanes	45
5.2 Alkyl-substituted arylphosphanes and arylalkylphosphanes.....	46
6 Conclusions.....	52
References	

1 Introduction

A coordination compound contains a metal center surrounded by a number of oppositely charged ions or neutral molecules (possessing lone pairs of electrons), which are known as ligands. The most straightforward way to affect the chemical behavior of a metal ion is through change in its ligands. It is well recognized that changes within the first coordination sphere of a metal ion can have a relatively dramatic impact on the properties of the entire complex, whereas modifications of the ligand substituents and superstructure have subtler and somewhat more predictable effects [1].

The most common ligand in organometallic chemistry is carbon monoxide, which may bond to a single metal or serve as a bridge between two or three metals. A variety of other ligands have been used, including diatomic ligands (nitrogen, nitrosyl), ligands containing linear or cyclic π -electron-systems (ethylene, butadiene, cyclopentadienyl, benzene), alkyl and acyl ligands, hydrogen, phosphites, and phosphanes [2,3]. The phosphanes are the ligands studied in this work.

There are fundamental similarities in the bonding of carbon monoxide, phosphanes, and alkenes to metals: with all there is σ -donation from a suitable ligand orbital to the metal center with concomitant π -back-bonding into an empty and suitable antibonding orbital of the ligand. In this work, carbon monoxide has a dual function; most importantly it is a substrate, but it also acts as a ligand, whereas phosphanes act as a ligand and alkenes act as important substrates as in many other catalytic reactions.[2]

Coordination compounds play an important role in homogeneous catalysis, where the organotransition metal catalyst and reagents are present in the same phase. In catalysis the coordination of substrates and loss of products must occur with low activation free energy, which means that the metal complexes must be labile [4]. These labile complexes are often coordinatively unsaturated in the sense that they contain a free coordination site or, at most, a site that is only weakly coordinated [4].

Designing new, modified phosphane ligands has become an art, important for the creation of highly effective and selective catalytic systems. Looking back to the past leaves no doubt that significant challenges remain for the future.

1.1 Phosphane ligands

Tertiary phosphanes of form PR_3 or $\text{PR}_2\text{R}'$ are usually prepared from phosphorus halides and organometallic reagents. Grignard reagents and organolithium reagents are commonly used as the organometallic reagent, but other metals (Al, Sn, Zn) have also found use [5]. The reactions are generally exothermic and are carried out at or below room temperature.

Phosphanes contain a lone electron pair at the phosphorus atom, which is used for the formation of a σ -bond with metals. π -Back-bonding from the d-orbitals of metals in low oxidation states is important in the case of electron-rich metals. The P–R σ^* -orbitals are utilized for π -back-bonding, and empty phosphorus 3d-orbitals also play a role—a role that is larger for ligands like trimethylphosphane than for trifluorophosphane [2,6,7,8,9,10,11,12]. The nature of the R groups attached to phosphorus thus determines the relative donor/acceptor ability of the ligand, and allows adjustment of the properties of the phosphane ligands [10,11].

Understanding of the ligand system is the first essential step toward catalyst design, since steric and electronic properties of the ligand can drastically influence the rate and selectivity of catalytic reactions. A large number of methods are available to study the stereoelectronic properties of phosphorus ligands and aid in the development of more efficient catalysts. In 1970 Tolman quantified steric and electronic properties in terms of cone angle (θ -value) and electronic parameter (χ -value) [13,14,15,16]. Subsequently other methods were developed for calculating the steric effects of ligands, which also take into account the variation in cone angle with ligand conformation [17,18]. Casey's natural biting angle has provided a useful tool for elucidating the steric properties of diphosphanes [19]. The quantification of electronic effects has continued, including investigations of parameters such as half neutralization potential for determination of ligand basicity [20,21], NMR chemical shifts and coupling constants [22,23,24,25], ionization potential [26,27], enthalpy of reaction [15,28,29,30], molecular electrostatic potential minimum V_{\min} [31] and the "aryl" effect E_{ar} [32,33,34].

Correlations have been sought among these parameters to evaluate steric and electronic effects. Generally, the correlations are limited to similarly modified ligands [22,31,35]. Correlations have been demonstrated between basicities and cone angles of the ligand series PMe_3 , PMe_2Ph , PMePh_2 , PPh_3 and $\text{P}(p\text{-tolyl})_3$, $\text{P}(m\text{-tolyl})_3$, $\text{P}(o\text{-tolyl})_3$, where basicity increased as the cone angle decreased [35]. Correlation between molecular electrostatic potential minimum V_{\min} and the Tolman electronic parameter, and also basicity, suggested that the V_{\min} parameter could be used as the σ -donating power of the phosphane ligand to a metallic moiety. If there was significant π -back-bonding from the metal to the phosphane, however, the correlation failed [31].

Triphenylphosphane (odorless solid) is probably the most widely used tertiary phosphane in homogeneous catalysis in part due to its ready availability and stability in air. Typically, trialkylphosphanes and mixed arylalkylphosphanes are liquids, air-sensitive, expensive, and nasty and noxious to handle—properties that may not recommend them for homogeneous catalysis [36]. Moreover, there are cases where they generate less active or even inactive analogues of arylphosphane-based catalysts [36]. The major difference between complexes containing trialkylphosphanes and triaryl-

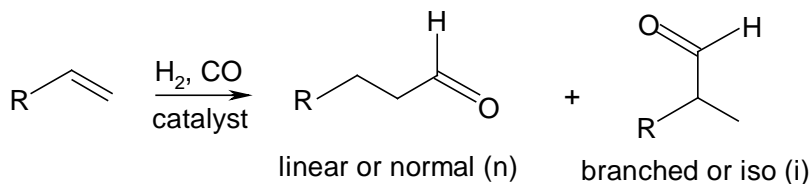
phosphanes is the greater σ -electron donor ability (basicity) of the trialkylphosphanes, which leads to the formation of more stable and less active low-pressure transition metal catalysts [37,38]. More recently, it has become apparent that rhodium trialkylphosphane complexes possess properties that make them suitable for a wide range of catalytic reactions [39]. Sometimes they are even the only systems available: for example, the much higher electron density on metal-containing trialkylphosphanes facilitates oxidative addition reactions, even of difficult substrates [39]. The branching of alkyldiarylphosphanes may improve both the i/n selectivity and the activity [40,37].

Most commercial homogeneous catalysts are based on phosphane complexes. Processes include hydrogenation, hydroformylation, hydrosilylation, hydrocyanation, and oligomerization [1,40,41,42,43]. The phosphanes with their ability to stabilize low oxidation states of transition metals, and especially the arylphosphanes with their greater steric bulk and weaker bonding affinity for metals relative to the alkylphosphanes, are ideal for the generation of an empty or potentially reactive coordination sites in the metal reaction sphere [1]. In addition, the good solubility of phosphane complexes, which can also be modified by changing the length of the alkyl substituent and introducing phenyl substituents, makes them highly attractive ligands for homogeneous catalysis. Lately, the synthesis of new water-soluble phosphane ligands such as sulfonated arylphosphanes, pyridylphosphanes, and phosphanes containing a nitrogen group have found industrially promising or relevant applications [44,45,46,47,48,49].

Evidently the first tertiary phosphane complex of a transition metal was described by Hoffmann as long ago as 1857. The triphenylphosphane ligand has a major role as a catalyst modifier for example in the famous Reppe compound $\text{Ni}(\text{CO})_2(\text{PPh}_3)_2$ used in alkene and acetylene polymerization, in the Wilkinson catalyst $\text{Rh}(\text{CO})(\text{Ph}_3\text{P})_3$ used in homogeneous hydrogenation of alkenes, acetylene, and carbonyl compounds, and in $\text{Rh}(\text{CO})(\text{PPh}_3)_{2\text{or}3}$ -type catalysts used in the hydroformylation of alkenes with hydrogen and CO [5].

1.2 Hydroformylation

Hydroformylation is the simultaneous addition of one mole each of hydrogen and carbon monoxide across a carbon-carbon double bond of alkene to produce linear and branched aldehydes having one more carbon atom than the original compound (Scheme 1). The reaction was discovered accidentally in 1938 by Otto Roelen. Although much progress has been made since then through the development of more efficient metal catalysts, hydroformylation continues to be the subject of innumerable studies, motivated by the need to increase the selectivity to linear or branched aldehydes, to reduce by-product formation, and to achieve milder and more environmentally friendly reaction conditions [40]. Today's hydroformylation plants operate with catalysts based on rhodium or cobalt, while platinum, palladium, and ruthenium catalysts are of research interest [40,50].



Scheme 1. Hydroformylation reaction.

The homogeneous hydroformylation reaction is one of the oldest processes making use of soluble transition metal catalysts and it is one of the largest volume of industrial applications of these catalysts. In the catalysts, the most extensively utilized ligands are phosphanes and carbon monoxide. Phosphane ligands offer several benefits over unmodified systems, including increased catalyst stability, improved reaction rates and selectivities, and enhanced partitioning into two-phase systems.[51,52,53]

Most of the seven million tons of aldehydes produced annually by this process are hydrogenated to alcohols or oxidized to carboxylic acids. Esterification of the alcohols produces plasticizers—the largest end-use. Detergents and surfactants make up the next largest category, followed by solvents, lubricants, and chemical intermediates. Asymmetric hydroformylation of several functionalised alkenes opens the way to production of chiral aldehydes, which can be used as a starting material for the synthesis of agro- and pharmaceutical chemicals.[40,41,51,45]

The most important hydroformylation process on industrial scale, propene hydroformylation, provides about 75% of all oxo chemicals consumed in the world [III]. Traditionally, the aim of this process has been to produce regioselectively the linear aldehyde, *n*-butanal. Via reactions to 2-ethylhexanol the *n*-butanal is converted to dioctyl phthalate, a plasticizer utilized in a wide range of PVC applications [40]. Recently, interest has focused on selective formation of the branched form, isobutanal, which now represents 9% of total production capacity and finds use in the production of polyols, such as neopentyl glycols [III].

2 Aims of the work

The present study was part of a project targeted at developing new rhodium catalysts for the propene hydroformylation reaction that would favor the formation of the branched aldehyde, isobutanal. The primary focus here was the preparation and characterization of new tertiary phosphane ligands and, while a second objective was to find trends in their behavior as catalytic ligands.

Steric and electronic properties of the phosphane ligand were modified with the aim of producing branched aldehydes in propene and 1-hexene hydroformylation. The first modifications were minor relative to the reference ligand triphenylphosphane, but as the work progressed the catalytically most promising features were combined with new modifying pieces. Some of the ligands have been reported earlier, but new preparation was essential to allow investigation of systematically modified groups of ligands. Additionally, most of the spectroscopic data for the ligands is new.

Publication I reports on trifluoromethyl-substituted phenylphosphanes. The main idea in introducing an electron-withdrawing substituent into the para or ortho position(s) was to increase the π -back-bonding from the rhodium atom to phosphorus atom and simultaneous to reduce the rhodium-to-carbonyl π -back-bonding of the *trans*-CO ligand. This would cause the CO molecule to be less strongly bonded to the rhodium center and facilitate alkene coordination. In the ortho position(s) the trifluoromethyl substituent also caused steric crowding.

Publications II-IV describe the steric modification of arylphosphane ligands through introduction of *ortho*-alkyl substituents to the aromatic group. The use of *ortho*-alkyl-substituted ligands was suggested by earlier finding in which (*o*-methylphenyl)diphenylphosphane ligand, as part of a platinum catalyst in the hydroformylation of 2-butene, exhibited enhanced selectivity to the branched aldehyde [54]. In this work the bulk of the alkyl group was increased step by step, from methyl to ethyl, isopropyl, and cyclohexyl.

Publication V was focused on *ortho*-alkyl-substituted arylalkylphosphanes. By combining the *ortho*-alkyl-substituted aryl group through the phosphorus atom with better σ -donor groups, the alkyls, we concomitantly modified the steric and electronic properties of phosphanes.

The third and fifth papers reported on investigations of hydroformylation reactions with *ortho*-alkyl-substituted pyridylphosphanes. The pyridyl ring(s) was chosen to be a

second modifying group since, in earlier investigations, the reaction rates obtained with pyridyl-modified compounds had been higher than the rates of their phenyl analogues. This has been attributed to the electron-withdrawing capacity of the pyridyl ring, which causes the CO molecule to be less strongly bonded to the rhodium center, thus facilitating alkene coordination [48,55].

Additionally, studies on sterically crowded polyaromatic monodentate phosphanes, anthryl- and naphthylphosphanes, are reported in the first, fourth, and fifth papers, since such ligands have rarely been studied in organometallic chemistry [56,57,58], let alone in hydroformylation reactions [59].

During the work it was noted that the catalytic properties of *meta*-alkyl-substituted triphenylphosphanes had not been extensively studied [60,61,62,63]. π -Electron density of the benzene ring is lower when this is substituted with electron-releasing alkyl group in *meta* position rather than in *ortho* or *para* position [64], and as a consequence the *meta*-alkyl-substituted phosphanes are poorer electron donor ligands than their *ortho* and *para* analogues. Use of *m*-alkyl-substituted phenylphosphanes as ligands also creates more space in the coordination sphere of a metal, though at the same time the steering effect is less than in the *ortho*-alkyl-substituted arylphosphanes. This work contains preliminary results of propene hydroformylation tests with three new *meta*-isopropyl-substituted phenylphosphanes.

Further, the synthesis and characterization of three unpublished chromium carbonyl complexes with arylphosphanes containing nitrogen heteroatom are reported for the first time in this publication. The compounds were synthesized to study the coordination chemistry of the prepared tertiary phosphane ligands.

Both the alkyl-substituted arylphosphane and alkyl-substituted mixed arylalkylphosphane ligands allowed comparative study of their properties and catalytic behavior, and correlations could be sought between spectroscopic and steric properties of the ligands and the hydroformylation results.

The catalytic properties of the ligands in hydroformylation were tested at the Helsinki University of Technology and the University of Joensuu. The modeling work and X-ray crystallographic work were carried out at the University of Joensuu. Some of the hydroformylation results are discussed here since properties of the modified phosphanes can be clarified through reference to their performance in catalysis.

3 Synthetic work

3.1 Reagents

Diethyl ether (Lab Scan) was distilled from sodium/benzophenone ketyl under nitrogen before use. Dichloromethane (Lab Scan), hexane (Lab Scan), ethanol (Altia), and methanol (Baker) were used without further purification or degassed with argon. H_2SO_4 (Reachim) and NaOH (FF-Chemicals) solutions were degassed with argon. $\text{Cr}(\text{CO})_6$ (Aldrich) and $(\text{CH}_3)_3\text{NO}\cdot 2\text{H}_2\text{O}$ (Fluka Chemica) were used as received. The other reagents were obtained from Aldrich, Lancaster, Merck, or Fluka and used without further purification.

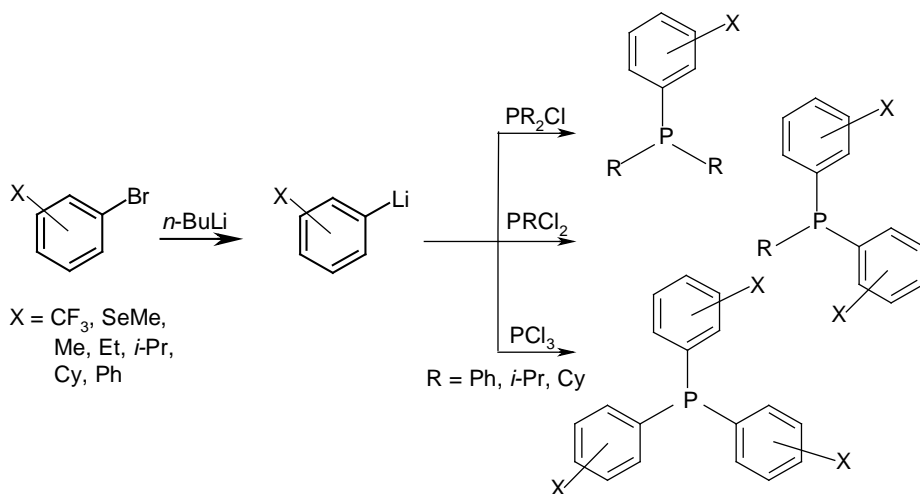
Analytical thin layer chromatography (TLC) was conducted on aluminium plates precoated with Kieselgel 60 F₂₅₄ silica gel (Merck). Column chromatography was carried out on degassed silica gel.

3.2 General procedure for preparation of phosphanes

Triphenylphosphane, a commercial phosphane ligand used in catalytic hydroformylation, was taken as the reference and starting point in varying the functionality of ligands. Modification was achieved by introducing trifluoromethylphenyl, selenomethylphenyl, 9-anthryl, alkyl-substituted phenyl and naphthyl, pyridyl, and alkyl groups as substituents at the phosphorus atom. Emphasis was on modification of the bulk and steric effects of phosphanes. As is well known, steric effects are not, however, easily distinguished from electronic effects.

The phosphane ligands were prepared mainly by the following procedure. Undiluted commercial solution of *n*-butyllithium (2.5 M solution in hexane) or a solution of *n*-butyllithium in diethyl ether was transferred dropwise via a canula to a freshly prepared solution of brominated organic reagent in diethyl ether at around 0°C. After several hours stirring, a solution of an appropriate chlorophosphane in diethyl ether was slowly added to the mixture of lithiated organic reagent and stirring was continued for a further few

hours. After slow warming to room temperature, solid and liquid layers were separated by filtration and solvent was removed in vacuum. Exceptionally, in the synthesis of pyridylphosphanes and (9-anthryl)phenylphosphanes, the reaction temperatures and reaction times were different from those described above. The reaction route is shown in Scheme 2.



Scheme 2. Reaction route for the preparation of substituted phosphanes.

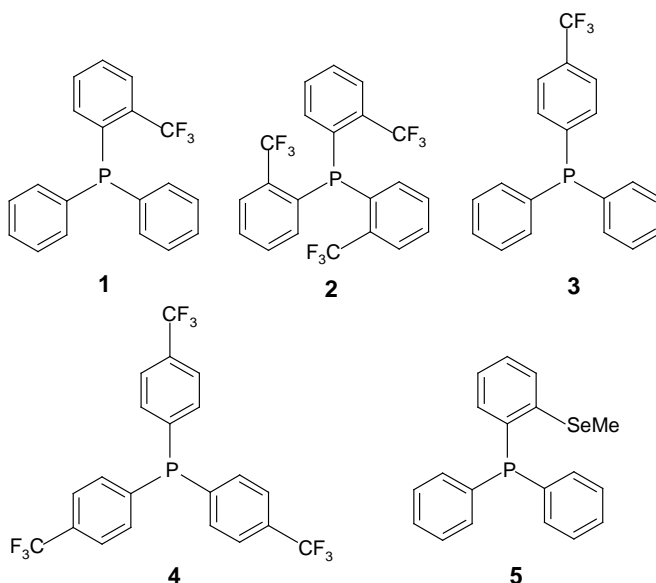
Halogenated arylphosphanes (Scheme 2) PPh_2Cl , PPhCl_2 , PCl_3 , $\text{P}(i\text{-Pr})_2\text{Cl}$, $\text{P}(i\text{-Pr})\text{Cl}_2$, and PCy_2Cl , are commercially available and widely used starting materials for the preparation of phosphane ligands. In addition to these, (2,5-dimethylphenyl)dichlorophosphane was synthesized by Friedel-Crafts reaction of phosphorus trichloride with *p*-xylene by earlier published literature methods and was used as starting material [65,66]. All reactions were performed in inert atmosphere with standard Schlenk techniques. The yields of the prepared ligands are presented in Table 1 section 4.2.1.

3.2.1 Trifluoromethyl- and selenomethyl-substituted phenylphosphanes¹

Trifluoromethyl- and selenomethyl-substituted phenylphosphanes were prepared in order to investigate the difference in effect of electron-withdrawing and electron-releasing groups in modifying arylphosphanes. Additionally, in the olefin hydroformylation, answers were sought to the question in which direction the functionality of substituents in phenylphosphanes should be modified for optimum performance.

First, hydroformylation tests were performed with known arylphosphanes containing an electron-releasing OMe-, SMe-, or NMe₂-substituted phenyl ring. The main interest here was the potential bidentate bonding from different donor atoms to the metal center [59,67,68]. Rhodium catalyst modified with the SMe-substituted phenylphosphane, (*o*-

thiomethylphenyl)diphenylphosphane, has produced improved results in the hydroformylation of MMA [59,68]. Trifluoromethyl-substituted phenylphosphanes **1-4** (Scheme 3) were prepared as a means of understanding in which way the electron-withdrawing functionality affects the hydroformylation results of olefins relative to the potentially bidentate ligands modified with electron-releasing functionality. Furthermore, a heterodonor phosphorus-seleno and electron-releasing ligand, (*o*-selenomethylphenyl)-diphenylphosphane **5**, was prepared and tested in the hydroformylation of olefins to supplement the series of above-mentioned heterodonor ligands.



Scheme 3. Schematic structures of (*o*-trifluoromethylphenyl)diphenylphosphane **1**, tris(*o*-trifluoromethylphenyl)phosphane **2**, (*p*-trifluoromethylphenyl)diphenylphosphane **3**, tris(*p*-trifluoromethylphenyl)phosphane **4**, and (*o*-selenomethylphenyl)diphenylphosphane **5**.

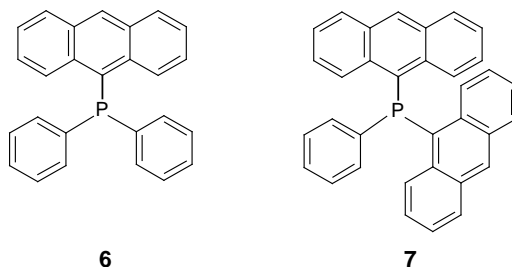
The synthesis of trifluoromethyl- and selenomethyl-substituted phenylphosphanes has been reported earlier [69,70,71,72]. The trifluoromethyl-substituted triphenylphosphane ligands (*o*-trifluoromethylphenyl)diphenylphosphane **1**, tris(*o*-trifluoromethylphenyl)phosphane **2**, (*p*-trifluoromethylphenyl)diphenylphosphane **3**, and tris(*p*-trifluoromethylphenyl)phosphane **4** (Scheme 3) were prepared from liquid 1-bromo-2-(trifluoromethyl)benzene or 1-bromo-4-(trifluoromethyl)benzene and the appropriate chlorophosphane, and likewise the (*o*-selenomethylphenyl)diphenylphosphane **5** (Scheme 3) was prepared from 1-bromo-2-(selenomethyl)benzene and diphenylchlorophosphane. Times for both reaction steps at 0°C were 1.5 h, and finally hydrolysis with hydrochloric acid (0.2 M) was carried out only with ligand **5** since the CF₃-substituted phenylphosphanes were known to oxidize easily and to convert slowly to the phosphane oxide during isolation from the reaction mixture [70]. The reaction of selenomethyl-substituted ligand **5** was also carried out at 0°C, because earlier the yield of tris(*o*-selenomethylphenyl)phosphane had not been improved when the reaction temperature was reduced to -78°C [72]. The

ligands **1-4** were washed with hexane, and ligand **5** was recrystallized from ethanol. The final solid products were brown (**1-2**), orange (**3-4**), and white (**5**).

3.2.2 (9-Anthryl)phenylphosphanes^I

Bulkier aromatic phosphanes containing anthryl ring(s) instead of phenyl ring(s) were synthesized in order to investigate the effect of steric stress on the catalytic activity and selectivity of the hydroformylation reaction.

The (9-anthryl)diphenylphosphane **6** and bis(9-anthryl)phenylphosphane **7** (Scheme 4) were synthesized according to the literature method of Wesemann *et. al.* [73]. A diethyl ether solution of 9-bromoanthryl was added to a solution of *n*-butyllithium in ether at -30°C . The mixture was stirred for 30 min, after which the appropriate chlorophosphane in diethyl ether was added over a period of 30 min. The resulting mixture was refluxed for 3.5 h and finally the cooled mixture was pumped dry in vacuum. The raw product was dissolved in dichloromethane and filtered over degassed Al_2O_3 (basic). The ligands were yellow solid products.



Scheme 4. Schematic structures of (9-anthryl)diphenylphosphane **6** and bis(9-anthryl)-phenylphosphane **7**.

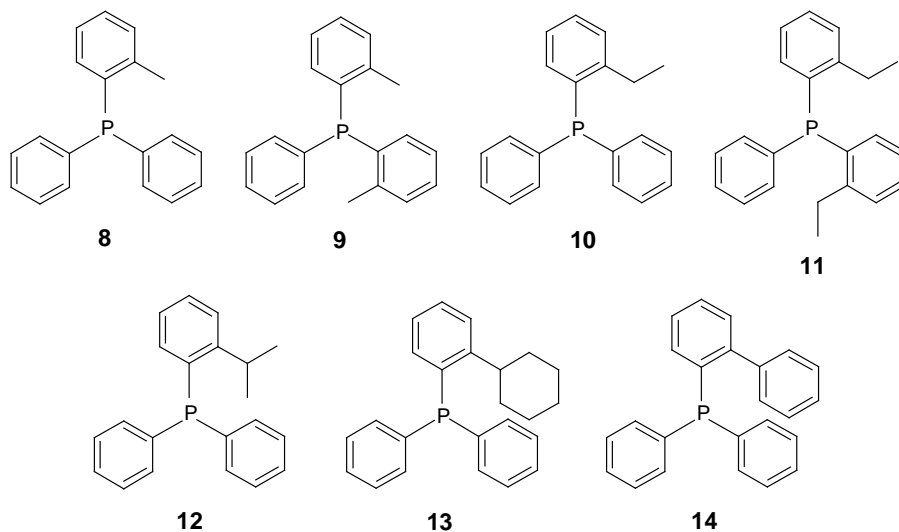
3.2.3 Alkyl-substituted arylphosphanes^{II, III, IV}

The modification of steric properties was continued by increasing the bulk of the arylphosphanes with *ortho*-alkyl substituents: the bulk of alkyl group was increased step by step from methyl to ethyl, isopropyl, and cyclohexyl. Functional groups were varied in the hope of finding relationships between the catalytic behavior and steric properties of the ligands since the *ortho*-alkyl-substituted ligands are electronically fairly similar.

All the phosphane ligands, (*o*-methylphenyl)diphenylphosphane **8**, bis(*o*-methylphenyl)phenylphosphane **9**, (*o*-ethylphenyl)diphenylphosphane **10**, bis(*o*-ethylphenyl)-phenylphosphane **11**, (*o*-isopropylphenyl)diphenylphosphane **12**, (*o*-cyclohexylphenyl)-diphenylphosphane **13**, and (*o*-phenylphenyl)diphenylphosphane **14** (see Scheme 5), were prepared by a modified literature method [74]. Undiluted solution of *n*-butyllithium reagent was added dropwise to a solution of brominated organic reagent in diethyl ether,

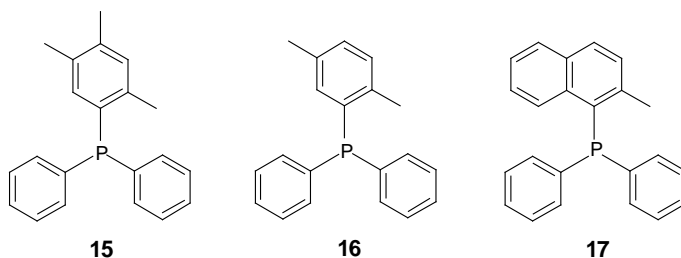
after which a solution of the appropriate chlorophosphane in diethyl ether was added. Times of both reaction steps at 0°C were two hours. The ligands were recrystallized from ethanol and as pure products they were white or translucent solids. Attempts to recrystallize ligand **10** were at first unsuccessful but after many attempts and an exceptionally long time (several weeks) was eventually achieved. Single crystals of **9-11** and **13** for X-ray crystallographic analysis were grown from a mixture of dichloromethane/hexane at room temperature. The *o*-phenyl-substituted phenylphosphane **14** was prepared to assess the difference in catalytic behavior between *o*-alkyl- and *o*-aryl-substituted ligands.

All the phosphane ligands introduced in this section, except **13**, have been mentioned in the literature [75,76,77]. However, it was considered to prepare all these ligands, with systematically increasing bulk, and as well to obtain a full range of spectroscopic and structural data for them.



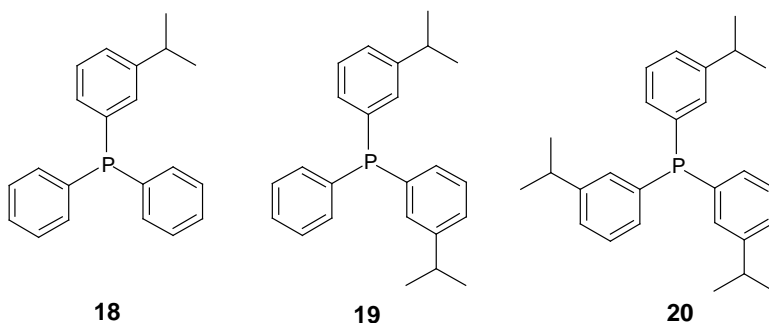
Scheme 5. Schematic structures of (*o*-methylphenyl)diphenylphosphane **8**, bis(*o*-methylphenyl)phenylphosphane **9**, (*o*-ethylphenyl)diphenylphosphane **10**, bis(*o*-ethylphenyl)phenylphosphane **11**, (*o*-isopropylphenyl)diphenylphosphane **12**, (*o*-cyclohexylphenyl)diphenylphosphane **13**, and (*o*-phenylphenyl)diphenylphosphane **14**.

The ligands (2,4,5-trimethylphenyl)diphenylphosphane **15** and (2,5-dimethylphenyl)diphenylphosphane **16** (Scheme 6) were prepared to find out how the presence of an *ortho*-alkyl substituent together with *meta*-alkyl and *para*-alkyl substituents and with a *meta*-alkyl substituent affect the hydroformylation results. Furthermore, (2-methylnaphthyl)diphenylphosphane **17** was prepared to combine the steric crowding of the polyaromatic ring with an *ortho*-methyl substituent. Ligands **15-17** were prepared like ligands **8-14** and the recrystallization from ethanol likewise gave white solid products. A different method has been reported for the synthesis of ligand **16**, but with lower yield and without NMR data [78].



Scheme 6. Schematic structures of (2,4,5-trimethylphenyl)diphenylphosphane **15**, (2,5-dimethylphenyl)diphenylphosphane **16**, and (2-methylnaphthyl)diphenylphosphane **17**.

Preparation of *meta*-alkyl-substituted phenylphosphanes was undertaken with the goal of achieving improved activity of the hydroformylation reaction. The newly prepared ligands (*m*-isopropylphenyl)diphenylphosphane **18**, bis(*m*-isopropylphenyl)phenylphosphane **19**, and tris(*m*-isopropylphenyl)phosphane **20** (Scheme 7) have the important bulky alkyl-substituent, but its steering role is less important in *meta* position.

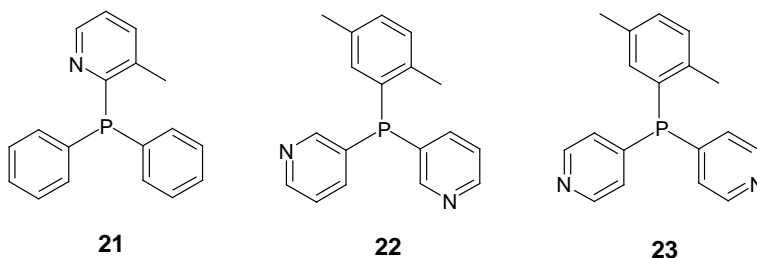


Scheme 7. Schematic structures of (*m*-isopropylphenyl)diphenylphosphane **18**, bis(*m*-isopropylphenyl)phenylphosphane **19**, and tris(*m*-isopropylphenyl)phosphane **20**.

Ligands **18-20** were prepared by the method described for *o*-alkyl-substituted phenylphosphanes. Lengthening of the time of the first reaction step to 3.5 h did not increase the yields. The ligands were purified by column chromatography on silica gel using dichloromethane/hexane (1:2) as eluent. The pure ligands **18-19** were translucent and oily, whereas the ligand **20** was a white solid. Single crystals of **18** for X-ray crystallographic determination were grown from a mixture of dichloromethane/hexane at room temperature.

3.2.4 Alkyl-substituted pyridylphosphanes^{III, V}

In compound **21**, (3-methyl-2-pyridyl)diphenylphosphane, the *o*-alkyl substituent was combined with pyridyl ring. *o*-Alkyl and pyridyl functions are in different side chains of the phosphane in ligands (2,5-dimethylphenyl)bis(3-pyridyl)phosphane **22** and (2,5-dimethylphenyl)bis(4-pyridyl)phosphane **23** (Scheme 8). The pyridyl ring was chosen to be a second modifying piece since pyridylphosphane catalysts have shown higher reaction rates than the corresponding phenylphosphanes, probably because of their stronger π -back-bonding character [48,55].



Scheme 8. Schematic structures of (3-methyl-2-pyridyl)diphenylphosphane **21**, (2,5-dimethylphenyl)bis(3-pyridyl)phosphane **22**, and (2,5-dimethylphenyl)bis(4-pyridyl)phosphane **23**.

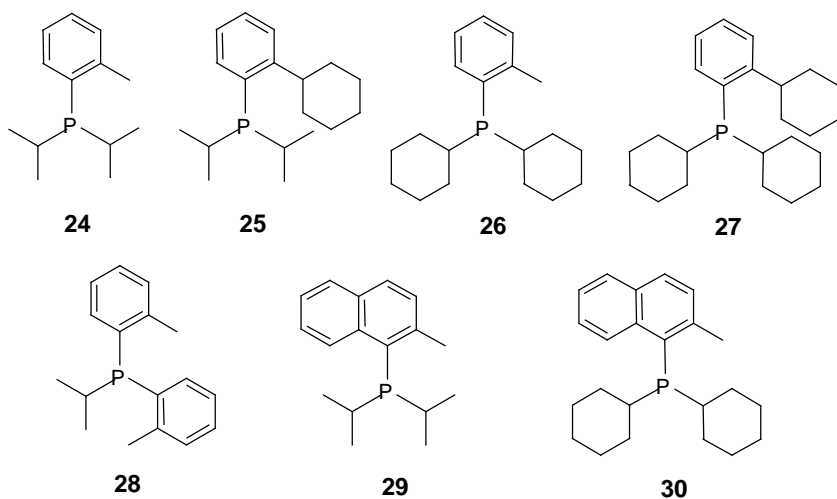
(3-Methyl-2-pyridyl)diphenylphosphane **21** was prepared according to the literature method by adding a solution of 2-bromo-3-methylpyridine in diethyl ether to a cooled solution of *n*-butyllithium in diethyl ether at -100°C [79]. The low reaction temperature, which was essential to decrease the formation of side products, was maintained by means of an ethanol/liquid nitrogen bath. After 1.5 h stirring, a solution of chlorodiphenylphosphane in diethyl ether was added and stirring was continued at -100°C for 1 h. After slow warming to room temperature, the raw product was extracted with sulfuric acid and the aqueous layer was separated and made alkaline with sodium hydroxide. The solid product was extracted back to the organic phase with diethyl ether and dried in vacuum. The ligand **21** has been mentioned in the patent literature [80].

Addition of TMEDA was essential to obtain ligands **22** and **23**. The syntheses were performed according to the method of Bowen *et al.* [81] by adding the appropriate 3- or 4-bromopyridine in diethyl ether to the cooled diethyl ether mixture of *n*-butyllithium and TMEDA at -115°C . After 5 min stirring, two thirds of the dichloro(2,5-dimethylphenyl)phosphane was added and stirring was continued for 0.5 h. The rest of the dichloro(2,5-dimethylphenyl)phosphane was then added and the mixture was stirred for a further 2.5 h at -100°C , before warming to room temperature overnight. The raw products were extracted and dried like ligand **21**. The products were purified by column chromatography on silica gel using dichloromethane/hexane/methanol (10:3:1) as eluent. Ligands **21** and **22** were white solids and **23** was transparent solid. Single crystals of **23** for X-ray crystallographic analysis were grown from dichloromethane/hexane mixture at room temperature.

3.2.5 *o*-Alkyl-substituted arylalkylphosphanes^V

Earlier studies on 1-hexene hydroformylation have shown that Rh-catalyst modified with linear trialkylphosphanes produce only alcohols, whereas the catalyst with triphenylphosphane or no phosphanes at all mainly form acetals [82]. The Rh-catalysts modified with triisopropylphosphanes promote the formation of aldehydes and the catalysts with mixed ethylphenylphosphanes the formation of mixtures of aldehydes and alcohols [82]. In other words, catalytic properties of alkylphosphanes are very much dependent on the site and degree of branching. In general, more stable metal complexes are formed with alkylphosphanes than with arylphosphanes owing to their greater σ -electron donor ability [37]. However, little attention has been paid to trialkylphosphane and mixed arylalkylphosphane rhodium complexes as catalysts for hydroformylation [39], it was to fill this gap that *ortho*-alkyl-substituted arylalkylphosphanes were prepared.

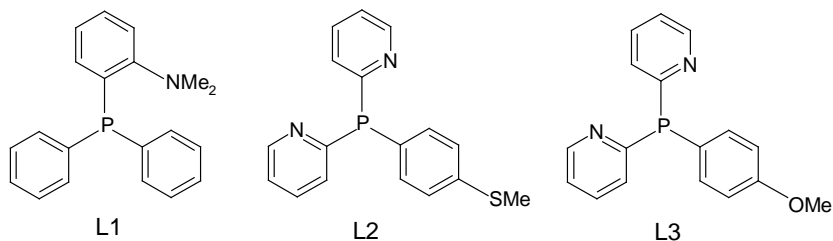
Isopropyl or cyclohexyl groups were combined with three different *ortho*-alkyl-containing aromatic groups—*o*-methylphenyl, *o*-cyclohexylphenyl, and 2-methylnaphthyl—giving the following ligands: (*o*-methylphenyl)diisopropylphosphane **24**, (*o*-cyclohexylphenyl)diisopropylphosphane **25**, (*o*-methylphenyl)dicyclohexylphosphane **26**, (*o*-cyclohexylphenyl)dicyclohexylphosphane **27**, bis(*o*-methylphenyl)isopropylphosphane **28**, (2-methylnaphthyl)diisopropylphosphane **29**, and (2-methylnaphthyl)dicyclohexylphosphane **30** (Scheme 9). The ligands were synthesized by the same method as the *o*-alkyl-substituted arylphosphanes but with use of the appropriate chloroalkylphosphanes. The ligands **24** and **29-30** were purified by column chromatography on silica gel using dichloromethane/hexane (1:2) as eluent, the ligands **26-27** were recrystallized from ethanol, the ligand **25** was washed with hexane, and **28** was dissolved in ethanol and filtered over silica gel. The pure ligands **24-25** and **28** were oily and translucent compounds, whereas **26-27** and **29-30** were white solids. Single crystals of **27** for X-ray crystallographic analysis were grown from dichloromethane/hexane mixture at room temperature.



Scheme 9. Schematic structures of (*o*-methylphenyl)diisopropylphosphane **24**, (*o*-cyclohexylphenyl)diisopropylphosphane **25**, (*o*-methylphenyl)dicyclohexylphosphane **26**, (*o*-cyclohexylphenyl)dicyclohexylphosphane **27**, bis(*o*-methylphenyl)isopropylphosphane **28**, (2-methylnaphthyl)diisopropylphosphane **29**, and (2-methylnaphthyl)dicyclohexylphosphane **30**.

3.3 Cr carbonyl derivatives of phosphane ligands containing nitrogen

The coordination chemistry of (*o*-*N,N*-dimethylaminophenyl)diphenylphosphane **L1**, (*p*-thiomethylphenyl)bis(2-pyridyl)phosphane **L2**, and (*p*-methoxyphenyl)bis(2-pyridyl)phosphane **L3** (Scheme 10) was studied here with chromium carbonyl derivatives in view of the earlier use of Cr(CO)₅L-type complexes to estimate the steric and electronic properties of phosphane ligands [17]. Changes in the electronic, steric, and geometric environments of ³¹P nuclei can be detected by means of the widely used and extremely sensitive ³¹P NMR spectroscopy measurements [83]. Ligands **L1** and **L2** have earlier been utilized in hydroformylation tests of MMA [59,68], and **L1** has been used to probe hydroformylation reactions of propene and 1-hexene [I].



Scheme 10. Schematic structures of (*o*-*N,N*-dimethylaminophenyl)diphenylphosphane **L1**, (*p*-thiomethylphenyl)bis(2-pyridyl)phosphane **L2**, and (*p*-methoxyphenyl)bis(2-pyridyl)phosphane **L3** used as ligands in the preparation of chromium carbonyl derivatives.

Chromium hexacarbonyl (1.00 mmol), ligand (1.00 mmol), and trimethylamine *N*-oxide dihydrate (1.00 mmol) were dissolved in 30 ml of dichloromethane and the resulting mixture was stirred at room temperature for 2 h. The solvent was removed in vacuum and the brown raw product was purified by column chromatography using silica gel as stationary phase. In the purification a mixture of dichloromethane/hexane (3:1) was used as eluent in the case of chromium carbonyl derivatives of (*o*-*N,N*-dimethylaminophenyl)diphenylphosphane (**L1**) and (*p*-methoxyphenyl)bis(2-pyridyl)phosphane (**L3**) and the above mentioned mixture and a mixture of methanol/dichloromethane (4:1) were used in the case of chromium carbonyl derivatives of (*p*-thiomethylphenyl)bis(2-pyridyl)phosphane (**L2**) ligand. The syntheses of ligands and their Cr carbonyl derivatives were carried out by earlier published methods [84,85,86].

In the purification, a yellow fraction was isolated when **L1** was used as ligand and yellow and red fractions were isolated when **L3** was used as ligand. In the case of Cr carbonyl derivatives containing ligand **L2**, purification with methanol/dichloromethane eluent gave yellow and brown fractions, whereas the dichloromethane/hexane eluent gave yellow and red fractions. However, after drying in vacuum and characterization, only one Cr carbonyl derivative of each ligand was verified. Single crystals for X-ray studies were grown from dichloromethane/hexane mixture. The crystals were orange for the complex of (*o*-*N,N*-dimethylaminophenyl)diphenylphosphane, yellow for the complex of (*p*-thiomethylphenyl)bis(2-pyridyl)phosphane, and red for the complex of (*p*-methoxyphenyl)bis(2-pyridyl)phosphane. The yields of the characterized chromium carbonyl derivatives are presented in section 4.3.2.

4 Characterization

4.1 Instrumentation and measurements

NMR spectroscopy: The phosphane ligands and chromium carbonyl derivatives were characterized with ^1H , $^{13}\text{C}\{^1\text{H}\}$, $^{31}\text{P}\{^1\text{H}\}$ NMR spectra, but with most of the ligands assistance in the interpretation was required from two-dimensional H,H-correlated COSY-90, H,C-correlated HSQC or C,H-correlated HETCOR, or long-range C,H-correlated COLOC NMR spectra. Most of the spectra were recorded on a Bruker DPX400 spectrometer at room temperature with deuterated chloroform (99.8% D, 0.03% TMS, Aldrich); a few of the ^1H NMR spectra were recorded on a Bruker AM200 spectrometer. The ^1H , $^{13}\text{C}\{^1\text{H}\}$ and two-dimensional NMR spectra were referenced to internal tetramethylsilane (TMS) and $^{31}\text{P}\{^1\text{H}\}$ NMR spectra to external 85% H_3PO_4 . Exceptionally, (2,5-dimethylphenyl)bis(3-pyridyl)phosphane and the chromium complex of (*p*-thiomethylphenyl)bis(2-pyridyl)phosphane were measured with deuterated acetone (99.9% D, Aldrich) because of solubility problems. The ^1H shifts were referenced to the residual signal of protons of partly deuterated acetone (2.05 ppm) and the ^{13}C shifts to the shift of deuterated acetone (30.5 ppm).

Mass spectrometry: Accurate masses were recorded with a Micromass LCT spectrometer using ESI+ method and a TOF mass analyzer.

X-ray crystallography: The X-ray measurements were performed with a Nonius KappaCCD diffractometer at the University of Joensuu. Further details of the measurements can be found in the original papers [I,II,V].

Quantum mechanical calculations: Geometrical arrangement and steric size of the free ligands were studied theoretically at the University of Joensuu by *ab initio* Hartree-Fock method using the 3-21G* basis set. The steric size of the free phosphane ligands was estimated by Tolman's cone angle method [16]. Further details of the modeling work can be found in the original papers [I-V].

4.2 Structure of phosphane ligands

The molecular masses of the prepared phosphanes were verified with measurements of accurate mass peaks. The structural characterization was based mainly on ^1H , $^{13}\text{C}\{^1\text{H}\}$, and $^{31}\text{P}\{^1\text{H}\}$ NMR techniques. In addition, to assign the ^1H and $^{13}\text{C}\{^1\text{H}\}$ NMR shifts two-dimensional H,H-correlated COSY-90, H,C-correlated HSQC or C,H-correlated HETCOR, or long-range C,H-correlated COLOC NMR spectra were needed, especially for the alkyl-substituted arylphosphanes and mixed arylalkylphosphanes. The molecular structures of successfully crystallized ligands **9–11**, **13**, **23**, and **27** were further determined by X-ray crystallography at the University of Joensuu. Qualitative pictures of the phosphane structures obtained from the quantum mechanical calculations carried out at the University of Joensuu were useful in the studies of activity and selectivity trends in hydroformylation reactions.

4.2.1 $^{31}\text{P}\{^1\text{H}\}$ NMR spectra and cone angles

The ^{31}P NMR shifts were characteristic for each of the phosphane ligand types (aromatic phosphanes, pyridylphosphanes, mixed arylalkylphosphanes). In general, as the substituents near the phosphorus atom became more sterically demanding, the ^{31}P nuclei experienced an increasing shielding effect and the phosphanes showed a shift from -2.6 to -27.7 ppm, while the cone angles increased from 149 to 223° . The ^{31}P NMR shifts, yields, and calculated cone angles of phosphane ligands **1–30** are presented in Table 1. The ^{31}P NMR resonances were singlets if not stated otherwise.

As expected, the ^{31}P nuclei of meta- or para-substituted phenylphosphanes (**18–20** and **3–4**) were deshielded ($\delta_{\text{p}} = -2.6$ to -4.3 ppm) relative to the ortho-substituted ones. The shielding effect caused by the *o*-alkyl substituents were also detected for the *o*-alkyl-substituted arylalkylphosphanes, whose ^{31}P NMR shifts in ppm were less than those of unsubstituted arylalkylphosphanes [87,88]. The shielding of the ^{31}P nuclei in polyaromatic phosphanes **6–7** and **17** was increased (low δ_{p} -values), whereas in the polyaromatic *o*-phenyl-substituted phenylphosphane **14** the shielding was lesser. The polyaromatic ligands have different electronic properties than the *o*-alkyl-substituted phenylphosphanes, including stronger ring current effect, which along with the steric bulk affected the ^{31}P NMR shift.

For monodentate phosphorus ligands the cone angle is defined as the apex angle of a cylindrical cone, centered at 2.28 \AA from the center of the phosphorus atom, which touches the outermost atoms of the model. For phosphanes containing different substituents an average for the three substituents is taken [41]. In general, the structures of free ligands are relatively flexible. Optimization of the *o*-substituted phosphanes mostly led to conformations where the substituents were located outside the cone. The *o*-methyl-substituted arylphosphanes (**8** and **17**) and *o*-alkyl-substituted mixed arylisopropylphosphanes (**24**, **25** and **29**) exhibited much lower steric repulsion than the others and the *o*-alkyl substituent of the ligands **8**, **17**, **24**, **25**, and **29** was located inside the cone.

Table 1. Yields, ^{31}P NMR shifts (δ_{P}), and calculated cone angles (θ) of ligands (L).

L	Name	Yield [%]	δ_{P} [ppm]	θ [°]
1	(<i>o</i> -trifluoromethylphenyl)diphenylphosphane	97	-9.4 (q, $^4J_{\text{PF}}$ 53 Hz)	174
2	tris(<i>o</i> -trifluoromethylphenyl)phosphane	92	-15.6 (q, $^4J_{\text{PF}}$ 55 Hz)	221
3	(<i>p</i> -trifluoromethylphenyl)diphenylphosphane	98	-4.1	149
4	tris(<i>p</i> -trifluoromethylphenyl)phosphane	68	-4.3	149
5	(<i>o</i> -selenomethylphenyl)diphenylphosphane	30	-10.4	-
6	(9-anthryl)diphenylphosphane	72	-22.9	176
7	bis(9-anthryl)phenylphosphane	61	-27.7	207
8	(<i>o</i> -methylphenyl)diphenylphosphane	53	-10.7	151
9	bis(<i>o</i> -methylphenyl)phenylphosphane	87	-19.0	158
10	(<i>o</i> -ethylphenyl)diphenylphosphane	50	-14.0	169
11	bis(<i>o</i> -ethylphenyl)phenylphosphane	71	-23.5	194
12	(<i>o</i> -isopropylphenyl)diphenylphosphane	23	-13.8	187
13	(<i>o</i> -cyclohexylphenyl)diphenylphosphane	72	-13.6	184
14	(<i>o</i> -phenylphenyl)diphenylphosphane	69	-11.9	191
15	(2,4,5-trimethylphenyl)diphenylphosphane	64	-11.8	159
16	(2,5-dimethylphenyl)diphenylphosphane	92	-9.5	159
17	(2-methylnaphthyl)diphenylphosphane	24	-16.5	223
18	(<i>m</i> -isopropylphenyl)diphenylphosphane	33	-2.6	161
19	bis(<i>m</i> -isopropylphenyl)phenylphosphane	30	-2.8	161
20	tris(<i>m</i> -isopropylphenyl)phosphane	58	-3.0	184
21	(3-methyl-2-pyridyl)diphenylphosphane	47	-6.3	151
22	(2,5-dimethylphenyl)bis(3-pyridyl)phosphane	30	-25.0	181
23	(2,5-dimethylphenyl)bis(4-pyridyl)phosphane	12	-15.7	-
24	(<i>o</i> -methylphenyl)diisopropylphosphane	35	-4.8	165
25	(<i>o</i> -cyclohexylphenyl)diisopropylphosphane	84	-4.4	172
26	(<i>o</i> -methylphenyl)dicyclohexylphosphane	82	-11.6	181
27	(<i>o</i> -cyclohexylphenyl)dicyclohexylphosphane	76	-14.6	211
28	bis(<i>o</i> -methylphenyl)isopropylphosphane	81	-22.3	198
29	(2-methylnaphthyl)diisopropylphosphane	41	6.6	199
30	(2-methylnaphthyl)dicyclohexylphosphane	66	-8.1	185

Mingos' statistical analysis has provided some interesting insights into the Tolman cone angle. Specifically, it has demonstrated that the cone angle in real complexes vary much more than previously believed and that there are systematic periodic differences in the average cone angles. The cone angles may also be affected by the steric requirements of the co-ligands and the coordination number of the complex. More surprisingly, the analysis suggests that even within a single complex containing two or more phosphane ligands the cone angle may vary considerably.[3]

The cone angles were larger in the free *ortho*-alkyl-substituted ligands than in their Rh(acac)CO(L) complexes, mainly because the phosphane ligands in Rh(acac)CO(L) complexes were surrounded by other ligands that caused steric pressure on the phosphane

side chains in the direction of the phosphane atom. For ligands **26** and **27**, the difference between the free and Rh(acac)CO(L)-coordinated ligand was about 10° [V]. In both the free and coordinated forms the *o*-alkyl-substituents of **26** and **27** were oriented outside the cone. In the case of ligands **8** and **17** the *o*-methyl substituent, which was oriented inside the cone in the free ligands, was oriented outside the cone in the Rh(acac)CO(L) coordinated state [IV]. The dissimilar orientation gave a 5° difference between the cone angles of the free and coordinated ligand **8** and as much as 64° for **17**.

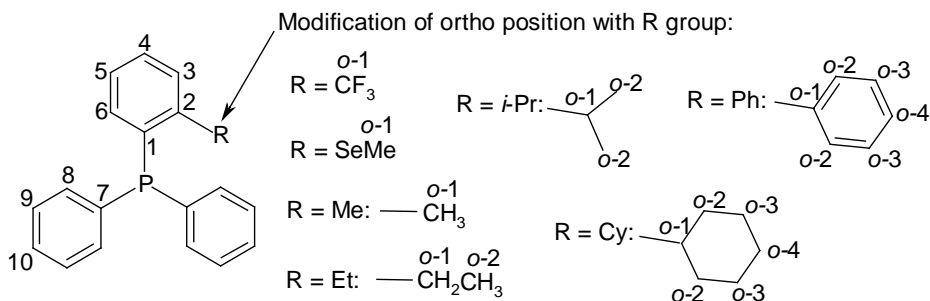
Although the above-mentioned statistical analysis and the results of the cone angle calculations based on optimized free ligand structures are not alone sufficient for the estimation of steric requirements of the coordinated ligands, they should give a qualitative idea of the steric size of the ligand. Moreover, in most cases the *ab initio* Hartree-Fock (HF) calculations and the determined X-ray crystal structures of the free ligands have indicated a similar orientation for the *o*-alkyl substituent. These results confirm the reliability of the HF calculations and make them valuable, particularly for the non-crystallizable phosphane ligands.

4.2.2 ^1H and $^{13}\text{C}\{^1\text{H}\}$ NMR spectra

The ^1H and $^{13}\text{C}\{^1\text{H}\}$ NMR spectra were characteristic for each type of phosphane. In general, the ^1H NMR shifts of aromatic and cyclohexyl spin systems were not of first order. This complicated the interpretation and even with the assistance of two-dimensional spectra the ^1H spectra could not be fully assigned. The $^{13}\text{C}\{^1\text{H}\}$ NMR spectra contained only a few overlapping and broad resonance peaks whose precise interpretation was not possible. Some differences in the ^1H and ^{13}C NMR shifts due to electronic and steric dissimilarities of the phosphanes are described in this section. The main emphasis is on the characterization of *o*-alkyl-substituted phenylphosphanes. NMR shifts of the *m*-isopropyl-substituted phenylphosphanes **18-20** and chromium carbonyl derivatives, which have not been published previously, are presented in detail.

4.2.2.1 *o*-Substituted arylphosphanes

The differences in the ^1H and ^{13}C NMR shifts of phosphane ligands modified with electron-withdrawing and electron-releasing functionality become clear in a comparison of the shifts of *o*-trifluoromethyl-substituted phenylphosphanes with those of *o*-selenomethyl-substituted and *o*-alkyl-substituted phenylphosphanes. The aromatic protons of electron-withdrawing *o*-trifluoromethyl-substituted ligands were mainly deshielded in relation to the protons of electron-releasing *o*-selenomethyl-substituted and *o*-alkyl-substituted ligands; for example, the shift of H⁶ was 7.2 ppm for ligand **1** and 6.8 ppm for ligands **5** and **8** (see Scheme 11 for numbering of hydrogen and carbon atoms).



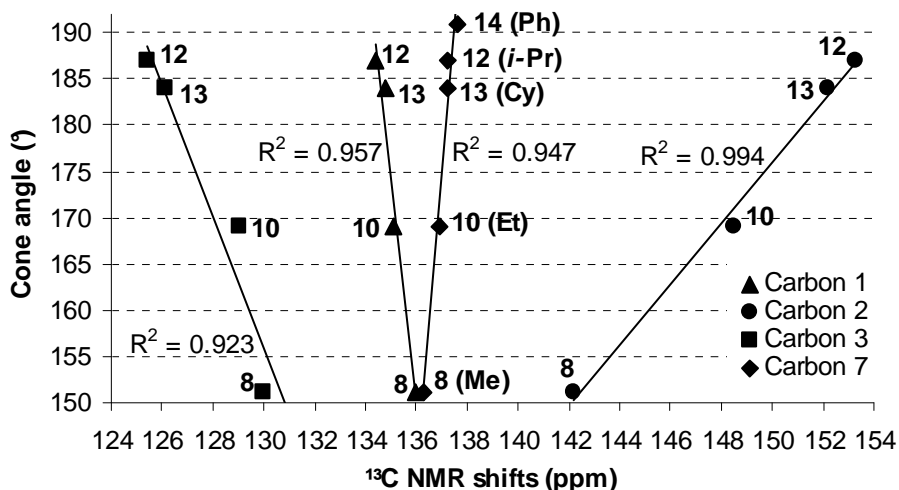
Scheme 11. Numbering of hydrogen and carbon atoms in NMR measurements.

The differences in the ^{13}C NMR shifts of the *o*-substituted phenyl ring are summarized in Table 2. The size of the *o*-alkyl substituent affected the ^{13}C NMR shifts of the substituted phenyl ring. The carbon C^2 in all the electron-releasing *o*-substituted arylphosphanes was least shielded, as expected, since generally the replacement of hydrogen by more electronegative carbon causes an increased δ_{C} -value of that deshielded carbon. The carbon C^1 was most shielded (lowest δ_{C} -value) in the *o*-(*i*-Pr)-substituted phenylphosphane (**12**) and least shielded (highest δ_{C} -value) in the *o*-SeMe-substituted phenylphosphane (**5**), whereas in *o*- CF_3 -substituted phenylphosphane (**1**) and *o*-alkyl-substituted phenylphosphanes (**8**, **10**, **13**) the shielding of carbon C^1 was between them. Relative to the shift of carbon C^3 of the *o*- CF_3 -substituted phenyl ring, the shifts of the *o*-Me- and *o*-Et-substituted phenyl rings were increased like the shifts of the *o*-SeMe-substituted phenyl ring, whereas the shifts of the *o*-(*i*-Pr)- and *o*-Cy-substituted phenyl rings were decreased. The shifts of carbons C^2 and C^4 - C^6 of all comparable *o*-alkyl-substituted phenylphosphanes were similar to those of *o*-selenomethyl-substituted phenylphosphane **5**. For these electron-releasing ligands (**5**, **8**, **10**, **12**, **13**) the carbon C^2 was deshielded (higher δ_{C} -value) and the carbons C^4 - C^6 were shielded (lower δ_{C} -value), in contrast to the carbons of electron-withdrawing ligand **1**.

Table 2. ^{13}C NMR shifts (ppm) for the *o*-substituted phenyl rings of phosphane ligands **1**, **5**, **8**, **13**, and **14**. *R* indicates the *o*-substituent of the phenyl ring. See Scheme 11 for numbering of carbon atoms.

δ_{C}	1 ($R = \text{CF}_3$)	5 ($R = \text{SeMe}$)	8 ($R = \text{Me}$)	13 ($R = \text{Cy}$)	14 ($R = \text{Ph}$)
C^1	136.6	139.2	136.0	134.8	135.9
C^2	134.9	139.3	142.2	152.2	148.4
C^3	126.4	130.0	130.0	126.1	130.1
C^4	131.6	129.4	128.6	129.0	127.3
C^5	128.9	126.2	126.0	125.9	127.2
C^6	136.1	133.4	132.7	133.4	134.1

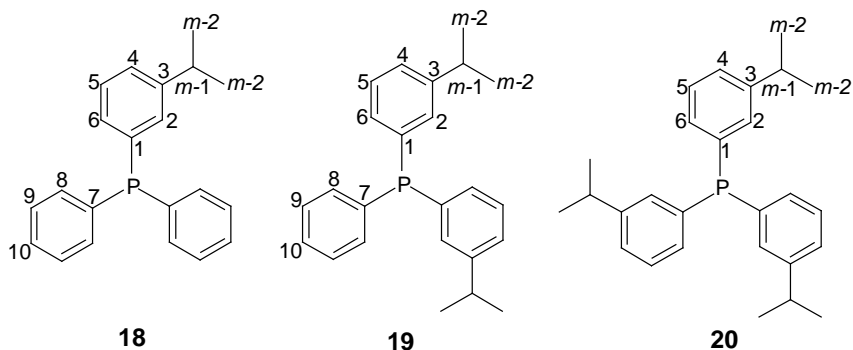
In general, as the *o*-alkyl-substituent became more bulky with both types of ligands (phenylphosphanes **8**, **10**, **12**, **13** and phenylalkylphosphanes **24-27**) the carbons C¹ and C³ showed a tendency to shielded shifts and carbons C² and C⁷ to deshielded shifts. The shifts of C¹, C² and C³ of the *o*-alkyl-substituted phenylphosphanes calculated from the empirical equations express this as well [89]. The tendency of the carbon C⁷ to deshield was also seen for the electronically different *o*-phenyl-substituted phenylphosphane **14**. The trends are illustrated in Scheme 12, in which the cone angles of the free ligands are used to characterize the steric size of the ligands created by the *o*-substituents. It should be noted, however, that although there is a correlation between the cone angle and the ¹³C NMR shifts of C¹-C³ there is no obvious dependence. Most likely, the shifts reflect the electronic effects caused by the particular *o*-alkyl substituent. This correlation is relevant, however, to the interpretation of the catalytic results below.



Scheme 12. Cone angle of the *o*-substituted phenylphosphanes (**8**, **10**, **12**, **13**, **14**) plotted as a function of the ¹³C NMR shifts of C¹, C², C³, and C⁷ (see Scheme 11). The *o*-substituent is shown in parentheses.

4.2.2.2 *m*-Isopropyl-substituted phenylphosphanes

The ¹H and ¹³C{¹H} NMR data for *m*-isopropyl-substituted phenylphosphanes **18-20**, which are reported here for the first time, are presented in Table 3, and the numbering of the hydrogen and carbon atoms is given in Scheme 13. The ¹H NMR resonances of protons H^{*m*-1} were septets and protons H^{*m*-2} were doublets, whereas the ¹H NMR resonances of aromatic spin systems were not of first order. In the ¹³C{¹H} NMR spectra, the shifts were doublets if the coupling constant are reported and singlets if not.



Scheme 13. Numbering of hydrogen and carbon atoms of ligands 18-20 in NMR measurements.

Table 3. ^1H and ^{13}C NMR shifts (ppm) and coupling constants (Hz) for the *m*-isopropyl-substituted phenylphosphane ligands 18-20. See Scheme 13 for numbering of hydrogen and carbon atoms.

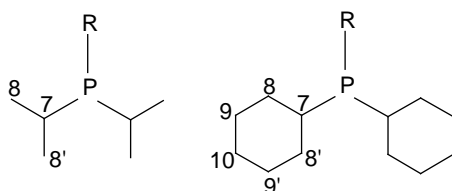
δ_{H}	δ_{C}	18		19		20	
J_{HH}	J_{CP}						
H^{m-1}	C^{m-1}	2.8	34.0	2.8	33.0	2.8	34.0
$^3J_{\text{HH}}$	-	7	-	7	-	7	-
H^{m-2}	C^{m-2}	1.2	23.9	1.2	23.9	1.2	23.9
$^3J_{\text{HH}}$	-	7	-	7	-	7	-
-	C^1	-	136.7	-	137.0	-	137.2
-	$^1J_{\text{CP}}$	-	10	-	10	-	10
H^2	C^2	7.2-7.3	132.3	7.2-7.3	132.1	7.2-7.3	132.0
-	$^2J_{\text{CP}}$	-	24	-	23	-	22
-	C^3	-	148.9	-	148.8	-	148.7
-	$^3J_{\text{CP}}$	-	8	-	8	-	7
H^4	C^4	7.2	126.8	7.2	126.8	7.2	126.7
H^5	C^5	7.2-7.3	128.4	7.2-7.3	128.4	7.2-7.3	128.3
-	$^3J_{\text{CP}}$	-	6	-	6	-	6
H^6	C^6	7.1	131.0	7.1	131.0	7.1	131.0
-	$^2J_{\text{CP}}$	-	15	-	16	-	16
-	C^7	-	137.4	-	137.7	-	-
-	$^1J_{\text{CP}}$	-	11	-	11	-	-
H^8	C^8	7.3	133.7	7.3	133.6	-	-
-	$^2J_{\text{CP}}$	-	19	-	19	-	-
H^9	C^9	7.2-7.3	128.4	7.2-7.3	128.3	-	-
-	$^3J_{\text{CP}}$	-	7	-	7	-	-
H^{10}	C^{10}	7.3	128.6	7.3	128.5	-	-

The ^1H NMR resonances appeared in the same region for all three *m*-isopropylphenylphosphanes (**18-20**). The ^1H shifts of H^2 , H^5 , and H^9 overlapped and appeared in the range 7.2 to 7.3 ppm. In the assignment of H^6 and H^2 , recording of the COSY spectrum was necessary where correlation peaks were observed between H^6 and H^5 and between H^5 and H^4 . This additional information made it possible to assign the shifts of C^2 and C^6 on the basis of HSQC spectra.

The shifts of aromatic carbons varied from 126.7 to 148.9 ppm. In general, the carbons C^2 - C^5 of the *m*-isopropyl-substituted phenyl ring and C^9 - C^{10} of the unsubstituted phenyl ring were shielded a little and carbons C^1 and C^7 deshielded as the number of *m*-isopropyl-substituted phenyl rings increased and the phosphanes became more bulky. The carbon C^3 gave a chemical shift in the lowest field at around 148.7 to 148.9 ppm.

4.2.2.3 Isopropyl and cyclohexyl groups directly bonded to phosphorus

The ^1H NMR data of the isopropyl groups directly bonded to phosphorus (ligands **24**, **25**, **29**) are presented in Table 4. The ^1H NMR shifts of the cyclohexyl groups appeared at 0.8 to 2.1 ppm for arylcyclohexylphosphanes **26**, **27**, and **30**; the exact peaks for the cyclohexyl groups could not be determined owing to the overlapping of signals. The $^{13}\text{C}\{^1\text{H}\}$ NMR data for phosphane ligands containing isopropyl or cyclohexyl groups directly bonded to phosphorus are presented in Table 5. In the $^{13}\text{C}\{^1\text{H}\}$ NMR spectra, the shifts were doublets if the coupling constants are reported and mainly singlets if not. As can be seen, for ligand **26** the shift of carbon C^7 was broad, while for ligand **27** it was partly overlapping with the shift of carbon C^{o-2} . Scheme 14 shows the numbering of the H and C atoms.



Scheme 14. Numbering of hydrogen and carbon atoms in NMR measurements. **R** means *o*-methyl- or *o*-cyclohexyl-substituted aryl ring.

Table 4. ^1H NMR shifts (ppm), multiplicities and coupling constants (Hz) for the isopropyl group directly bonded to phosphorus. See Scheme 14 for numbering of hydrogen and carbon atoms.

δ_{H}	$J_{\text{HH}}, J_{\text{HP}}$	24	25	29
H^7		2.1 (dsep)	2.1 (dsep)	2.7 (broad)
	$^3J_{\text{HH}}$	7	7	-
	$^2J_{\text{HP}}$	2	2	-
H^8		0.9 (dd)	0.9 (dd)	0.7 (dd)
	$^3J_{\text{HH}}$	7	7	7
	$^3J_{\text{HP}}$	12	12	14
$\text{H}^{8'}$		1.1 (dd)	1.1 (dd)	1.3 (dd)
	$^3J_{\text{HH}}$	7	7	7
	$^3J_{\text{HP}}$	15	15	17

Table 5. ^{13}C NMR shifts (ppm) and coupling constants of doublets (Hz) for isopropyl and cyclohexyl groups directly bonded to phosphorus. See Scheme 14 for numbering of hydrogen and carbon atoms.

δ_{C}	J_{CP}	24	25	26	27	29	30
C^7		24.1	24.2	~33.7	~34.5	25.5	35.8
	$^1J_{\text{CP}}$	13	13	-	-	14	13
C^8		19.3	19.3	29.0	29.3	21.2	30.5
	$^2J_{\text{CP}}$	11	11	7	8	14	11
$\text{C}^{8'}$		20.2	20.3	30.3	30.8	23.0	33.5
	$^2J_{\text{CP}}$	19	19	14	17	29	25
C^9		-	-	27.1	27.2	-	27.0
	$^3J_{\text{CP}}$	-	-	9	7	-	8
$\text{C}^{9'}$		-	-	27.2	27.3	-	26.9
	$^3J_{\text{CP}}$	-	-	13	12	-	13
C^{10}		-	-	26.4	26.5	-	26.4

The COLOC NMR spectra, which were measured only for the *o*-alkyl-substituted aryldialkylphosphanes **24**, **27**, and **29**, showed long-range $^{13}\text{C}-^1\text{H}$ ($^3J_{\text{CH}}$) couplings and the nonequivalent carbons C^8 and $\text{C}^{8'}$ and correspondingly C^9 and $\text{C}^{9'}$ were possible to assign on the basis of these couplings. Such long-range coupling is possible only if the two nuclei belong to the same alkyl group. Thus, in the isopropylphosphane ligands **24**, **25**, and **29**, and in the cyclohexylphosphane ligands **26**, **27**, and **30**, the two alkyl groups directly bonded to phosphorus are equivalent to each other. Earlier unsubstituted phenyldiisopropylphosphane [90] and phenyldicyclohexylphosphane [88,91,92] have showed similar magnetic nonequivalency of the carbons and protons as well. Assignment of ^{13}C NMR shifts of the isopropyl and cyclohexyl carbons in the ligands **24**, **25**, **26**, **27**, and **29** agreed with the earlier published shielding order $\delta(\text{C}^7) > \delta(\text{C}^{8'})$, $\delta(\text{C}^8) > \delta(\text{C}^{9'})$, $\delta(\text{C}^9) > \delta(\text{C}^{10})$ [91]. The $^2J_{\text{CP}}$ and $^3J_{\text{CP}}$ values for $\text{C}^{8'}$ and $\text{C}^{9'}$ were considerably larger than those for C^8 and C^9 as has been noted for unsubstituted phenyldicyclohexylphosphane

[90,91,92]. Apparently, the observed nonequivalency of the protons and carbons in the NMR spectra of the *o*-alkyl-substituted aryldialkylphosphanes was a consequence of steric crowding. Therefore, the rotation around the P–C bonds was rather restricted in the NMR timescale.

4.2.3 X-ray crystal structures

Ligands **9**, **10**, **11**, **13**, **18**, **23**, and **27** formed single crystals, whose X-ray crystal structures were determined at the University of Joensuu. The bond distances and angles of the structures were in the predictable range; in general, there were only minor differences in the bond angles and distances. The X-ray crystal structures of ligands **9**, **18**, **23**, and **27** are presented in Figure 1.

In all structures with a single alkyl substituent in ortho position of the phenyl ring, the substituent was located outside the cone owing to the steric demands (see ligands **9** and **27** in Fig. 1). The *m*-isopropyl substituent (ligand **18**) was oriented analogously. In the crystal structure of (2,5-dimethylphenyl)bis(4-pyridyl)phosphane **23** the *m*-methyl substituent was coordinated inside the cone and the *o*-methyl substituent outside the cone.

The COLOC NMR spectra of ligands **24**, **27**, and **29** indicated that carbons C⁸ and C^{8'} were magnetically nonequivalent (see Scheme 14). In the crystal structure of ligand **27**, the nonequivalency of carbons C⁸ and C^{8'} was observed in one of the cyclohexyl rings directly bonded to phosphorus, where the C⁸–C⁷–P and C^{8'}–C⁷–P angles were dissimilar (109.42° and 117.93°). In the other cyclohexyl ring the angles were almost equal (108.49° and 109.97°). The dissimilarity may have an effect on the NMR spectra if the rotation around the P–C bonds has become limited in the NMR timescale.

In the free ligand state and in both Rh-coordinated complexes, Rh(CO)(Cl)(L)₂ and Rh(acac)CO(L), the *o*-alkyl substituent was similarly oriented outside the cone close to the Rh-center [II,V]. Apparently, in most cases the crystal structure of the free ligand gives a qualitatively picture of the orientation of the *o*-alkyl-substituent in the Rh-coordinated complexes and so can assist in the prediction of catalytical behavior. However, sterically smaller *o*-alkyl substituents (like methyl) can more easily orientate inside the cone than can bulkier substituents and it is riskier to use their crystal structures to estimate the orientation of the smaller size *o*-substituent in metal complexes.

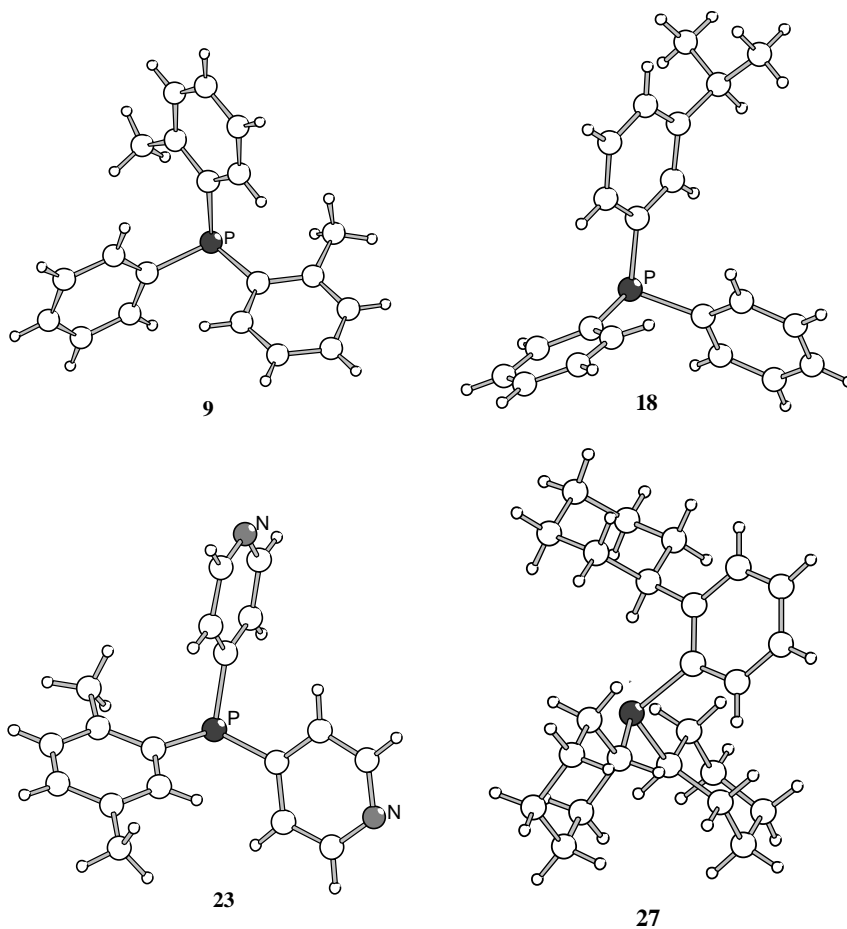


Fig. 1. Crystal structures of bis(*o*-methylphenyl)phenylphosphane **9**, (*m*-isopropylphenyl)diphenylphosphane **18**, (2,5-dimethylphenyl)bis(4-pyridyl)phosphane **23**, and (*o*-cyclohexylphenyl)dicyclohexylphosphane **27**.

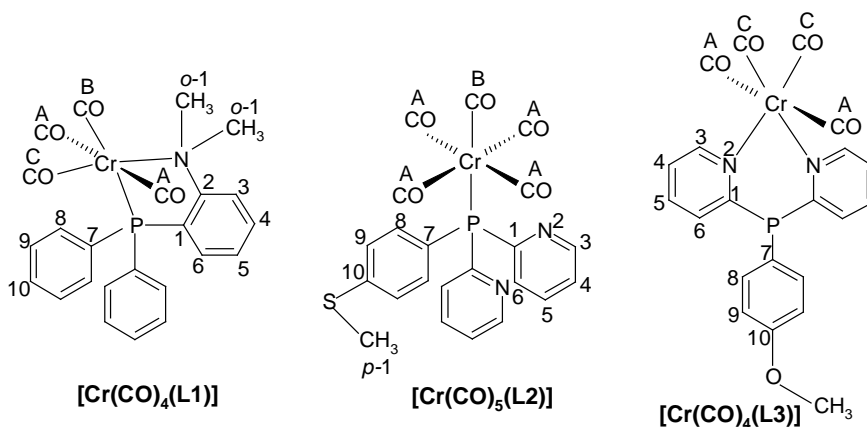
4.3 Structure of Cr carbonyl derivatives

The molecular masses of the chromium carbonyl derivatives were verified from their mass spectra. In addition to the X-ray crystal structures, the characterization of the Cr complexes of (*o*-*N,N*-dimethylaminophenyl)diphenylphosphane and (*p*-thiomethylphenyl)bis(2-pyridyl)phosphane ligands was based on ^1H , $^{13}\text{C}\{^1\text{H}\}$, $^{31}\text{P}\{^1\text{H}\}$, and H,C-correlated HSQC NMR techniques. The spectra of the free ligands and the shifts of the free ligands calculated with empirical equations assisted in the interpretation of NMR

spectra of the complexes [68,84,85,89]. The assignments of the CO resonance peaks of the complexes were based on the ^{13}C signal intensity ratios and the magnitude of the C–P coupling constants. The Cr complex of (*p*-methoxyphenyl)bis(2-pyridyl)phosphane decomposed rapidly in deuterated chloroform and did not give interpretable NMR spectra. After the measurement its color was also changed, to light turquoise.

4.3.1 NMR spectra

The ^1H and $^{13}\text{C}\{^1\text{H}\}$ NMR data for the unpublished chromium complexes of (*o*-*N,N*-dimethylaminophenyl)diphenylphosphane [$\text{Cr}(\text{CO})_4(\text{L1})$] and (*p*-thiomethylphenyl)bis(2-pyridyl)phosphane [$\text{Cr}(\text{CO})_5(\text{L2})$], hitherto unpublished, are presented in Table 6. The numbering of the hydrogen and carbon atoms for these complexes and for [$\text{Cr}(\text{CO})_4(\text{L3})$] is shown in Scheme 15. The ^1H NMR shifts for the methyl protons were singlets, while the aromatic resonances were not of the first order. In the $^{13}\text{C}\{^1\text{H}\}$ NMR spectra, the shifts were doublets if the coupling constants are reported and singlets if not.



Scheme 15. Numbering of hydrogen and carbon atoms of Cr complexes of (*o*-*N,N*-dimethylaminophenyl)diphenylphosphane (L1), (*p*-thiomethylphenyl)bis(2-pyridyl)phosphane (L2), and (*p*-methoxyphenyl)bis(2-pyridyl)phosphane (L3).

Table 6. ^1H and ^{13}C NMR shifts (ppm) and coupling constants (Hz) for (*o*-*N,N*-dimethylaminophenyl)diphenylphosphane (L1), $\text{Cr}(\text{CO})_4(\text{L1})$, (*p*-thiomethylphenyl)bis(2-pyridyl)phosphane (L2), and $\text{Cr}(\text{CO})_5(\text{L2})$.

δ_{H}	δ_{C} J_{CP}	L1		$\text{Cr}(\text{CO})_4(\text{L1})$		L2		$\text{Cr}(\text{CO})_5(\text{L2})$	
H^{o-1}	C^{o-1}	2.6	45.5	3.1	59.9	-	-	-	-
-	$^4J_{\text{CP}}$	-	4	-	-	-	-	-	-
H^{p-1}	C^{p-1}	-	-	-	-	2.5	14.8	2.5	14.9
-	C^1	-	134.5	-	160.7	-	164.1	-	160.1
-	$^1J_{\text{CP}}$	-	10	-	32	-	4	-	60
-	C^2	-	158.0	-	161.0	-	-	-	-
-	$^2J_{\text{CP}}$	-	19	-	22	-	-	-	-
H^3	C^3	7.2-7.4	120.5	7.5-7.6	119.5	8.7	150.9	8.8	150.2
-	$^3J_{\text{CP}}$	-	-	-	9	-	12	-	17
H^4	C^4	7.2-7.4	129.8	7.5-7.6	131.8	7.1-7.2	123.3	7.3	123.7
-	$^4J_{\text{CP}}$	-	-	-	2	-	-	-	2
H^5	C^5	7.0	124.4	7.3	127.1	7.6	136.2	7.7	135.8
-	$^3J_{\text{CP}}$	-	-	-	4	-	-	-	6
H^6	C^6	6.8	134.2	7.3	133.7	7.1-7.2	128.9	7.3	127.4
-	$^2J_{\text{CP}}$	-	-	-	-	-	20	-	17
-	C^7	-	138.2	-	135.2	-	132.3	-	129.4
-	$^1J_{\text{CP}}$	-	12	-	38	-	10	-	38
H^8	C^8	7.2-7.4	133.7	7.5-7.6	132.6	7.4	136.6	7.5	133.6
-	$^2J_{\text{CP}}$	-	19	-	12	-	3	-	11
H^9	C^9	7.2-7.4	128.2	7.4-7.5	128.7	7.1-7.2	126.6	7.3	125.7
-	$^3J_{\text{CP}}$	-	4	-	10	-	9	-	10
H^{10}	C^{10}	7.2-7.4	128.3	7.4-7.5	130.0	-	142.1	-	142.4
-	$^4J_{\text{CP}}$	-	-	-	2	-	-	-	2
-	A	-	-	-	218.2	-	-	-	216.6
-	$^2J_{\text{CP}}$	-	-	-	13	-	-	-	13
-	B	-	-	-	225.1	-	-	-	222.2
-	$^2J_{\text{CP}}$	-	-	-	3	-	-	-	6
-	C	-	-	-	228.7	-	-	-	-
-	$^2J_{\text{CP}}$	-	-	-	13	-	-	-	-

Because of the coordination of nitrogen to the metal center, the H^{o-1} and C^{o-1} of methyl groups in the P,N-coordinated bidentate complex $[\text{Cr}(\text{CO})_4(\text{L1})]$ were deshielded in relation to the corresponding nuclei of the free ligand. The $^4J_{\text{CP}}$ coupling constant of carbon C^{o-1} was not observed for the coordinated form. Coordination of L1 also affected the other coupling constants: $^2J_{\text{CP}}$ of C^8 decreased, $^3J_{\text{CP}}$ of C^9 increased, while $^3J_{\text{CP}}$ of carbons C^3 and C^5 and also $^4J_{\text{CP}}$ of C^{10} and C^4 became observable. Moreover, the coordination of phosphorus to the metal center caused a clear 26 Hz increase in the $^1J_{\text{CP}}$ coupling constant of C^7 and a 22 Hz increase in the $^1J_{\text{CP}}$ of C^1 . The carbon C^7 directly bonded to phosphorus showed about 3.0 ppm shielding relative to the free ligand, whereas the carbon C^1 was deshielded and appeared at 160.7 ppm.

The $^{13}\text{C}\{^1\text{H}\}$ spectrum of the bidentate $[\text{Cr}(\text{CO})_4(\text{L1})]$ complex exhibited three carbonyl doublets, indicating the presence of three types of carbonyls, one trans to phosphorus (225.1 ppm, $^2J_{\text{CP}}$ 3 Hz), one trans to nitrogen (228.7, $^2J_{\text{CP}}$ 13 Hz), and one cis to both phosphorus and nitrogen (218.2 ppm, $^2J_{\text{CP}}$ 13 Hz). $^2J_{\text{CP}}$ coupling constants of the carbonyl groups followed the earlier noticed trend in which the coupling of carbonyls cis to phosphorus was higher than the coupling of carbonyl trans to phosphorus $|^2J_{\text{CP}(\text{cis})}| > |^2J_{\text{CP}(\text{trans})}|$ [93].

The ^{31}P NMR shift was clearly increased upon coordination of the ligand L1 to the metal center: δ_{P} was -12.5 ppm for the free ligand and 58.3 ppm for the P,N-coordinated $[\text{Cr}(\text{CO})_4(\text{L1})]$ complex. Typically, the ^{31}P NMR shift of phosphorus-bound bidentate complexes is around 25 to 32 ppm deshielded relative to the corresponding monodentate P-coordinated complexes [94].

In the monodentate complex $[\text{Cr}(\text{CO})_5(\text{L2})]$ the shifts of H^{p-1} and C^{p-1} appeared almost unchanged relative to the free ligand L2. Coordination of L2 affected the coupling constants as well: the $^2J_{\text{CP}}$ coupling constant of C^6 decreased, $^2J_{\text{CP}}$ of C^8 increased, $^3J_{\text{CP}}$ of carbons C^3 and C^9 and also $^1J_{\text{CP}}$ of C^7 increased, and $^3J_{\text{CP}}$ of C^5 and $^4J_{\text{CP}}$ of C^4 and C^{10} became observable. Moreover, the coordination of phosphorus to the metal center caused a huge 56 Hz increase in the $^1J_{\text{CP}}$ coupling constant of C^1 , and an increase of 28 Hz in the $^1J_{\text{CP}}$ of C^7 . The shift of C^1 showed 4.0 ppm shielding relative to the free ligand.

The $^{13}\text{C}\{^1\text{H}\}$ spectrum of the monodentate complex $[\text{Cr}(\text{CO})_5(\text{L2})]$ exhibited two carbonyl doublets, at 216.6 ppm and 222.2 ppm, due to the carbonyls oriented trans and cis to phosphorus. $^2J_{\text{CP}}$ coupling constants of the carbonyl groups followed the same trend as for the P,N-coordinated complex: $|^2J_{\text{CP}(\text{cis})}|$ (13 Hz) $>$ $|^2J_{\text{CP}(\text{trans})}|$ (6 Hz) [93].

The ^{31}P NMR shift was clearly increased upon coordination of the ligand L2 to the metal center: for the free ligand δ_{P} was -1.6 ppm and for the P-coordinated $[\text{Cr}(\text{CO})_5(\text{L2})]$ complex 63.4 ppm.

4.3.2 X-ray crystal structures

The X-ray crystal structures were consistent with the NMR spectra, showing the phosphane ligand to have replaced one or two of the carbonyl ligands. The structures of complexes $[\text{Cr}(\text{CO})_4(\text{L1})]$, $[\text{Cr}(\text{CO})_5(\text{L2})]$, and $[\text{Cr}(\text{CO})_4(\text{L3})]$ showed slightly distorted octahedral geometry (Figure 2). The carbonyl ligands trans to phosphorus or nitrogen had a slightly shortened Cr–C bond relative to the cis-carbonyls. The Cr–N bond lengths were slightly shorter than the Cr–P bond lengths. The Cr–P bond of the bidentate complex $[\text{Cr}(\text{CO})_4(\text{L1})]$ was 2.329 Å and the Cr–N bond was 2.279 Å. For the monodentate complex $[\text{Cr}(\text{CO})_5(\text{L2})]$ the Cr–P bond was 2.371 Å, and for the bidentate $[\text{Cr}(\text{CO})_4(\text{L3})]$ complex the Cr–N bonds were 2.155 Å and 2.157 Å. Complexation caused some changes in the bond angles. For example, in the bidentate complex $[\text{Cr}(\text{CO})_4(\text{L1})]$ the angle P–Cr–N was 81.7° and in the complex $[\text{Cr}(\text{CO})_4(\text{L3})]$ the angle N–Cr–N was 85.5° . The angles also induced deviations in the other angles, the carbonyl ligands being pushed away from the phosphane ligands.

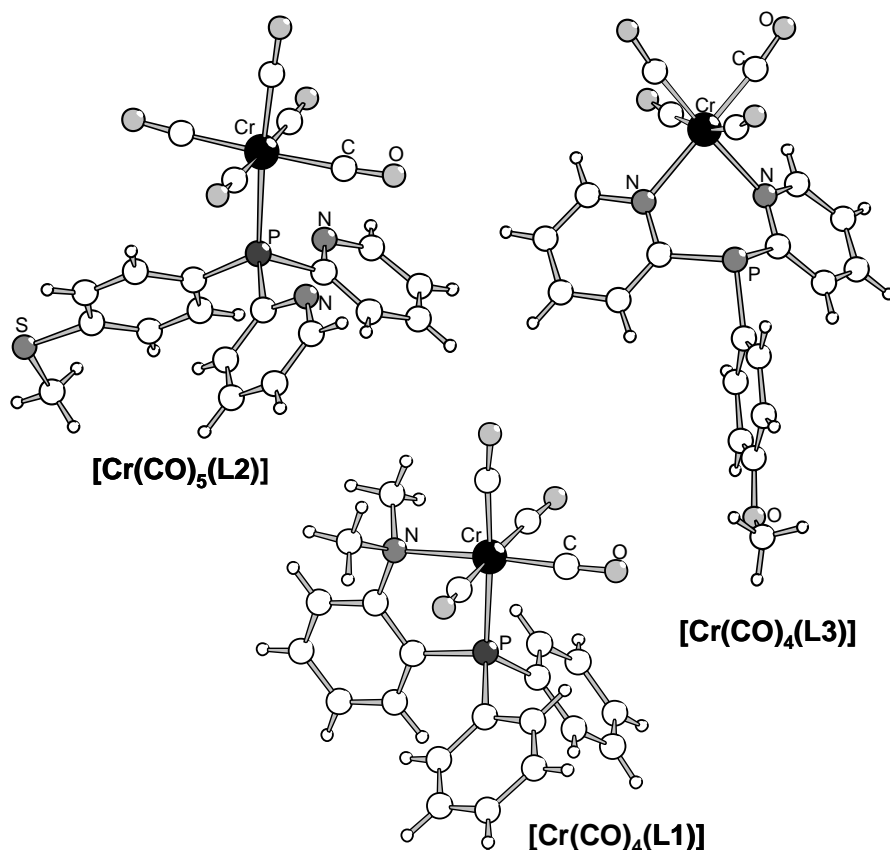


Fig. 2. Crystal structures of monodentate $[\text{Cr}(\text{CO})_5(\text{L2})]$ and bidentate $[\text{Cr}(\text{CO})_4(\text{L1})]$ and $[\text{Cr}(\text{CO})_4(\text{L3})]$ complexes.

The structure of the P,N-coordinated $[\text{Cr}(\text{CO})_4(\text{L1})]$ complex was analogous with the bidentate structure of the P,S-coordinated Cr complexes of *o*-thiomethyl-substituted phenylphosphane [86]. The closely related pyridylphosphane ligands L2 and L3 coordinated monodentately and bidentately. It was interesting that two such similar ligands showed different coordination modes. In fact, purification of the two complexes with dichloromethane/hexane eluent gave yellow and red fractions and only the yellow fraction obtained in the preparation of the ligand L2 complex $[\text{Cr}(\text{CO})_5(\text{L2})]$ could be characterized. Both NMR and X-ray crystal structure methods showed it to be monodentate. The few incidentally crystallized single crystals of the red fraction obtained in the preparation of ligand L3 complex were identified in X-ray crystal structure determination as complex $[\text{Cr}(\text{CO})_4(\text{L3})]$. The yields of the crystallized complexes were as follows: 82% for orange $[\text{Cr}(\text{CO})_4(\text{L1})]$, 33% for yellow $[\text{Cr}(\text{CO})_5(\text{L2})]$, and 6% for red $[\text{Cr}(\text{CO})_4(\text{L3})]$.

5 Hydroformylation

Besides the reaction conditions, the reactivity of a transition metal center strongly depends on the donor/acceptor properties and steric crowding of the ligands bound to it. Tailoring of the catalyst sphere through sophisticated ligand design allows steering of the selectivity and activity of the catalysts.

Earlier in Rh-catalyzed hydroformylation studies with electronically modified *p*-CF₃-, *p*-OMe-, and *p*-NMe₂-substituted triphenylphosphanes, the rates of the 1-hexene hydroformylation reaction were found to increase with slightly decreasing *i/n* ratios as the electron density on the rhodium atom was reduced by electron-withdrawing functionality on the modifying phosphane ligand [95,96]. Pyridylphosphanes have shown a similar tendency for hydroformylation rates [48,55]. On the other hand, phosphane ligands such as alkylphosphanes, which have greater σ -electron donor ability (more basic ligands), have in general been found less active since their dissociation requires higher reaction temperatures [37].

Increasing the steric crowding of phosphorus ligands through the addition of *o*-alkyl substituents of triphenylphosphite [97,98,99,100] or triphenylphosphane [54,101] or branched/cyclic alkyl groups of alkylphosphane or mixed alkylphenylphosphane [82,37,38] has increased iso-selectivities and, in the case of aromatic ligands, also reaction rates in olefin hydroformylation. It has been suggested that bulky ligands favor low coordination numbers and, thus, the coordinative unsaturation of the metal center becomes greater favoring branched products [40,97,98,99,100,102].

The phosphane ligands of this work were designed to increase the *i/n* ratio in propene or 1-hexene hydroformylation. In the 1-hexene process isomerization is unavoidable, yielding the internal olefins 2- and 3-hexene [103]. The internal olefins, which are less reactive, predominantly form branched products, 2-methylhexanal and 2-ethylpentanal [103,104]. Previous investigations on 1-hexene isomerization have shown that a sterically bulky phosphane ligand or several triphenylphosphane ligands bound to rhodium center hinder the coordination of olefins to a metal center and decrease isomerization [105,106]. Additionally, donor-acceptor properties of the phosphane ligands affect the electron density of the metal center and thereby the mode and the strength of the coordination of olefins [105,106].

The 1-hexene hydroformylation tests were carried out at the University of Joensuu and the propene hydroformylation tests at the Helsinki University of Technology. Ms. Merja Harteva has carried out the preliminary propene hydroformylation tests of *m*-isopropyl-substituted phenylphosphanes (**18-20**). In both cases the phosphane ligands were combined *in situ* with the rhodium precursors. The reaction conditions in the 1-hexene hydroformylation were as follows: p = 15 bar [I,II] or 20 bar [V] or 25 bar [IV], T = 80°C [I,II,IV] or 100°C [V] or 120°C [II], precursor = Rh₄(CO)₁₂ [I,II] or Rh(acac)(CO)₂ [IV,V], L/Rh = 5 [V] or 10 [I,II] or 50 [IV], 1-hexene/Rh = 815 [II,IV] or 10 000 [I,V]. Reaction conditions in the propene hydroformylation were: p = 10 bar (CO/H₂ = 1), T = 100°C, precursor = Rh(NO₃)₃, L/Rh = 10, and propene/Rh = 512 [IV-V] or 2250 [III] or 3200 [I].

In the 1-hexene hydroformylation tests, the sterically bulky arylphosphane and mixed arylalkylphosphane ligands did not suppress the isomerization activity in the manner earlier observed with bulky tri-*n*-butylphosphane ligand [106]. The donor–acceptor properties of these phosphanes are dissimilar, which means that the ligands have a different effect on the electron density of the metal center, and probably both the mode and the strength of the coordination of 1-hexene were dissimilar. Optimization of the reaction conditions in 1-hexene hydroformylation was both complicated and time consuming. In part because of that, high isomerization activity was associated with most of the ligands and, apparently, affected the *i/n* ratios. Even so, in the final stage of the work improved reaction conditions with five of the ligands afforded better chemoselectivity to the aldehydes 2-methylhexanal and 1-heptanal [IV].

The main challenge in propene hydroformylation was to obtain high iso-selectivity with reasonably high initial rate. The properties of the *o*-alkyl-substituted phosphanes, which produced best iso-selectivity, are discussed in more detail, and, reasons for the catalytic behavior are sought in the structural parameters of the ligands.

The propene hydroformylation reaction studied with *o*-alkyl-modified phosphanes was sometimes carried out in different propene-to-rhodium ratio, which complicates the comparison of the results. However, the reference ligand (PPh₃) was tested under all the reaction conditions and the PPh₃ results reveal when the comparison is out of line. Comparison of the catalytic results should give a general indications of the properties of the studied phosphane ligands.

5.1 Trifluoromethyl- and selenomethyl-substituted phenylphosphanes¹

Even though the main purpose of the CF₃ substituents was to modify the electronic state of the phosphorus atom, the ortho-substitution in ligands **1** and **2** also affected the cone angles of the ligands. The ligands **1** and **2** behaved alike in the hydroformylation by blocking those reactions that most likely were due to steric reasons.

The Rh-catalysts modified with *p*-CF₃-substituted phosphane **4** showed selectivities for the branched aldehydes at the same levels as PPh₃; however, the aldehydes were minor products. The conversions in hydroformylation reactions were for both propene and 1-hexene fairly high. The closely similar ligand **3**, in turn, blocked the

hydroformylation reactions entirely. The reason for this unexpected behavior is not clear, but handling errors are suggested since ligand **3** oxidized easily in accurate mass peak measurement.

The catalytic behavior of *o*-SeMe-substituted phenylphosphane (ligand **5**) was similar to that of the potentially bidentate *o*-SMe- and *o*-OMe-modified ligands: all three blocked the propene hydroformylation reaction. *p*-SMe-Modification and *o*-NMe₂-modification, on the other hand, produced *n*-butanal as the main product. Consistent with the potential bidentate coordination mode of *o*-SMe- and *o*-NMe₂-modified phosphanes [107], the behavior of *o*-SeMe might also explained in terms of bidentate coordination to the rhodium center.

5.2 Alkyl-substituted arylphosphanes and arylalkylphosphanes^{II-V}

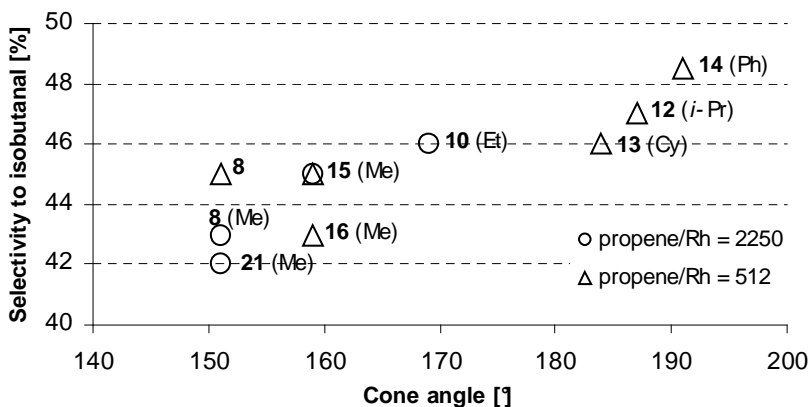
The selectivity to isobutanal was increased at the cost of activity with all the *o*-alkyl-substituted aryl- and arylalkylphosphanes as well as with (*o*-phenylphenyl)diphenylphosphane (**14**).

The iso-selectivities (S_i) of Rh-catalysts modified with *meta*-isopropyl-substituted phenylphosphanes (**18-20**) in propene hydroformylation were comparable with the selectivity of the catalyst modified with PPh₃ ($S_i = 36\%$). The catalysts modified with *o*-alkyl-substituted phosphanes and the *o*-phenyl-substituted phenylphosphane (**14**) showed highest selectivity to branched aldehyde isobutanal ($S_i = 42-53\%$), except for the (2-methylnaphthyl)dialkylphosphanes (**29, 30**: $S_i = 35\%$ and 33% , respectively). In the improved reaction conditions for 1-hexene hydroformylation, the selectivity to branched 2-methylhexanal was higher for Rh-catalysts modified with the *o*-substituted arylphosphanes (**12-14, 16-17**, $S_i = 26-32\%$) than for the PPh₃-modified catalyst ($S_i = 24\%$) [IV]. However, the effect of the modified ligands on branching was less than for propene. Polyaromatic anthrylphosphanes **6-7** without *o*-alkyl-substituent did not promote the formation of branched aldehydes [I]. Evidently the *o*-substituents of arylphosphanes near the coordination sphere of rhodium have a significant steering effect in the propene hydroformylation, the electronically different, bulky *o*-alkyl-substituted polyaromatic phosphane ligands, such as the the (2-methylnaphthyl)dialkylphosphanes (**29 and 30**), interfere with the formation of branched isobutanal.

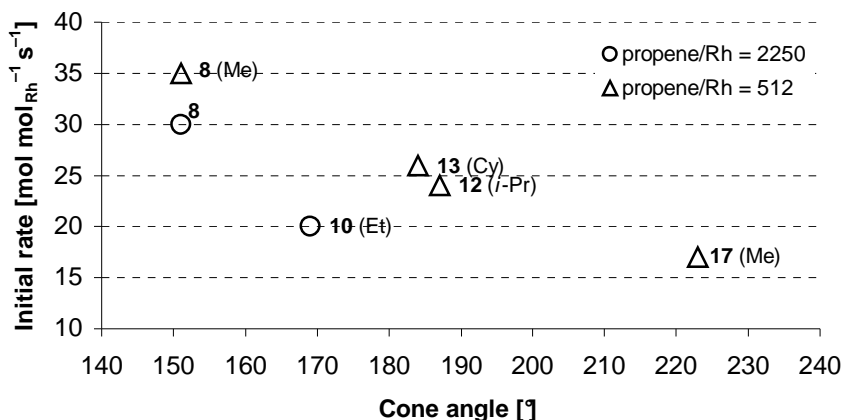
The initial rates and conversions for propene hydroformylation were more unpredictable than the selectivities. Initial rates and conversions were highest when the Rh-catalyst was modified with PPh₃ (53 and 45 mol mol_{Rh}⁻¹ s⁻¹ when the propene/Rh ratio was 2250 and 512, respectively, conversion 98-99%). Moreover, in preliminary tests *m*-isopropyl-substituted phenylphosphanes (**18-20**) increased the initial rate of propene hydroformylation even up to the level of the reference ligand PPh₃ and also showed good conversions. The Rh-catalysts modified with (*o*-alkylphenyl)diphenylphosphanes (**8, 10, 12-13, 15-16**) gave higher initial rates (20-35 mol mol_{Rh}⁻¹ s⁻¹) than the mixed (*o*-alkylphenyl)dialkylphosphanes (**24-25, 27**: 12-17 mol mol_{Rh}⁻¹ s⁻¹). Likewise, the conversions of the (*o*-alkylphenyl)diphenylphosphanes (63-70%) were higher than the mixed (*o*-alkylphenyl)dialkylphosphanes (35-52%). The *o*-alkyl-substituent containing pyridylphosphanes **21-23** [III, V] and the *o*-phenyl-substituted phenylphosphane **14** gave lower

initial rates in propene hydroformylation than the *o*-alkyl-substituted phenylphosphanes. These initial rates of the pyridylphosphanes were in contrast to earlier observations in 1-octene hydroformylation [48,55]. With the improved reaction conditions, the conversion in 1-hexene hydroformylation was as much as 90 to 99% when the catalyst was modified with *o*-substituted arylphosphanes **13**, **14**, or **17** compared with 82% for PPh₃ [IV]. The steric crowding of bis(*o*-alkylphenyl)diphenylphosphanes (**9**, **11**) and the greater σ -donor ability of mixed bis(*o*-methylphenyl)isopropylphosphane (**28**) and (2-methylnaphthyl)-dialkylphosphanes (**29-30**) almost blocked the propene hydroformylation reaction and the initial rates were only about 2 to 5 mol mol_{Rh}⁻¹ s⁻¹). The bulky *o*-substituent reduces the initial rate of propene hydroformylation, but altering of the electronic effects of the *o*-substituents and changing the two unsubstituted phenyl groups to the alkyl groups directly bonded to phosphorus—*isopropyls* or *cyclohexyls*—have more unpredictable suppressing effects. Relative to *o*-alkyl-substituted phenylphosphanes the *m*-isopropyl-substituted phenylphenylphosphanes allow more space for the substrate in the coordination sphere of rhodium, but they also have less ability to release electron density to the phosphorus atom [64]. For these reasons the *m*-isopropyl-substituted phenylphosphanes have higher initial rates than *o*-alkyl-substituted phenylphosphanes in propene hydroformylation but are less capable of steering the reaction toward branched isobutanal.

The parameters of *o*-substituted arylphosphane ligands investigated for the description of catalytic behavior in propene hydroformylation were the cone angle, the ³¹P NMR shift and the ¹³C NMR shifts. Calculated cone angles are a measure of the steric properties of the ligands and do not characterize any electronic effects variations of phosphane ligands. Note, however, that the cone angles of closely related phosphanes may correlate with the ¹³C NMR shifts (Scheme 12 in section 4.2.2.1). Schemes 16 and 17 show that the selectivity increases and the initial rate decreases as the cone angle of *o*-substituted arylphosphane increases. However, even minor electronic changes such as 2,5-dimethyl-substitution of the phenyl ring (ligand **16**) can cause a deviation in the selectivity pattern (Scheme 16). Electronic modifications of the ligands have a still more unpredictable effect on the initial rate (Scheme 17) and a trend is seen only for closely related ligands whose steric bulk has increased step by step (**8**, **12**, **13**, **17**).

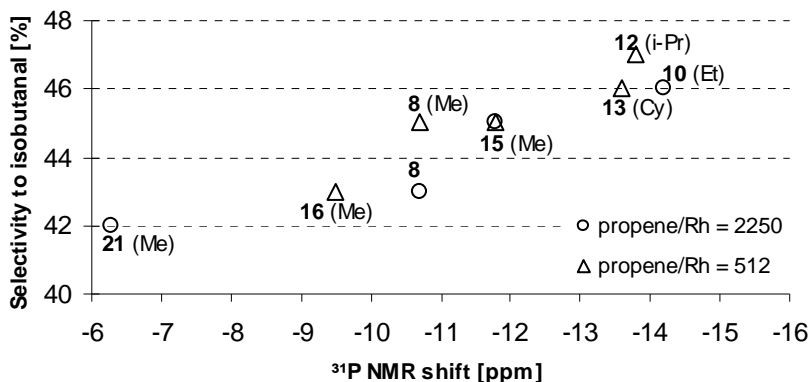


Scheme 16. Selectivity to isobutanol plotted as a function of cone angle. The values are for *o*-substituted arylphosphanes. The substituent is shown in parentheses.

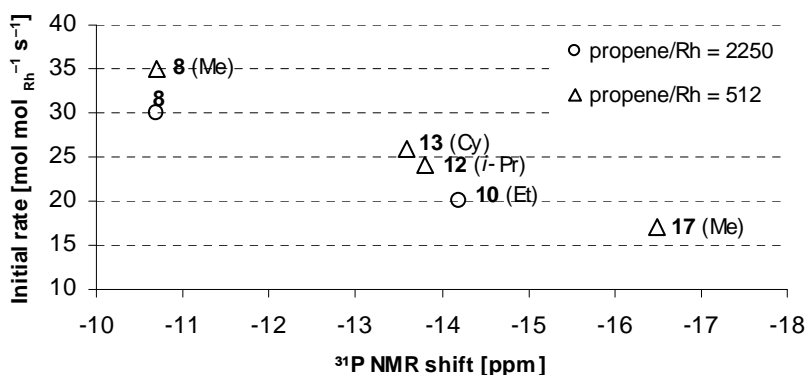


Scheme 17. Initial rates of propene hydroformylation reaction plotted as a function of cone angle. The values are for *o*-alkyl-substituted arylphosphanes. The substituent is shown in parentheses.

Besides the electronic properties of the ligand, the ^{31}P NMR shift reflects the spatial surrounding of the phosphorus atom. Schemes 18 and 19 show that the selectivity increases and the initial rate decreases as the ^{31}P NMR shift of *o*-alkyl-substituted arylphosphanes decreases. *o*-Phenyl-substituted ligand **14** was off the chart of selectivity (Scheme 18), apparently, because the out of cone oriented phenyl substituent altered the electronic effect (such as gave stronger ring current effect), which affected the ^{31}P NMR shifts differently than did the *o*-alkyl substituent. As in the case of cone angles, (Scheme 17), a correlation between the ^{31}P NMR shifts and initial rates is observed for the closely related phosphanes. Even the electronically altered *o*-methyl-substituted naphthylphosphane **17** seems to fit the trend (Scheme 19).



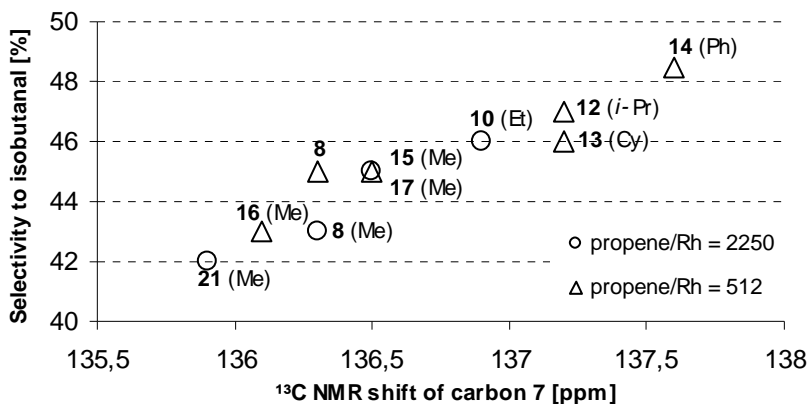
Scheme 18. Selectivity to isobutanal plotted as a function of ³¹P NMR shifts. The values are for *o*-alkyl-substituted arylphosphanes. The substituent is shown in parentheses.



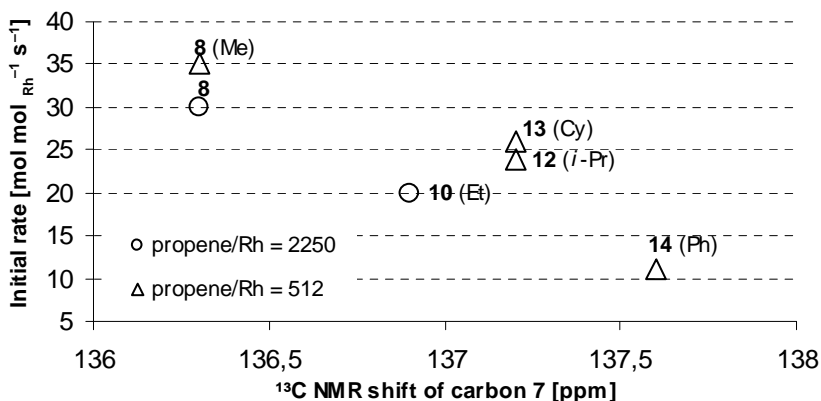
Scheme 19. Initial rates of propene hydroformylation reaction plotted as a function of ³¹P NMR shifts. The values are for *o*-substituted arylphosphanes. The substituent is shown in parentheses.

The ¹³C NMR shift of C⁷ (see Scheme 11 for numbering of carbons) is an indirect measure of the stereoelectric state of the phosphane ligand and, simultaneously, it seems to correlate linearly with the cone angles of the closely related *o*-substituted phenylphosphane ligands (**8**, **10**, **12**, **13**, and **14**; Scheme 12). The ring current effect is less important in ¹³C NMR spectroscopy [108] and the extra ring current effect created by polyaromatic groups could thus be neglected in the case of the C⁷ shift. Furthermore, the carbon C⁷ may be less affected by the steric effects of bulky *o*-substituents than is the phosphorus atom. The shift of the polyaromatic ligand **14** appears in both correlations (Schemes 20 and 21). However, the initial rate of the polyaromatic ligand **17** does not fit in the initial rate trend of *o*-substituted phenylphosphanes. Evidently, the bulkier naphthyl group reduces the initial rate more drastically than the steric bulk of the *o*-substituents.

Analogously, the anthryl groups of ligand **7** weakened the conversion in propene hydroformylation [I].



Scheme 20. Selectivity to isobutanol plotted as a function of the ¹³C NMR shift of C⁷ (see Scheme 11 for numbering of carbons). The values are for *o*-substituted arylphosphanes. The substituent is shown in parentheses.



Scheme 21. Initial rates of propene hydroformylation reaction plotted as a function of the ¹³C NMR shift of C⁷ (see Scheme 11 for numbering of carbons). The values are for *o*-substituted arylphosphanes. The substituent is shown in parentheses.

All the parameters discussed in this section could be expected to correlate more or less linearly with the catalytic results of catalyst systems modified with a still wider group of closely related *o*-alkyl-substituted phenylphosphanes. In the case of the parameter δ_{C^7} even the electronically dissimilar ligand **14** fit in the correlations with initial rate and selectivity to isobutanol. At the same time, the fit of the dissimilar ligands **15**, **16**, **17**, and **21** in some of the correlations must be considered coincidence at this time given the limited results for these kinds of ligands.

The parameters discussed above allow a rough prediction of the catalytic properties of sterically and electronically closely related phosphane ligands. The findings also show that separation of the steric and electronic effects of phosphane ligands is hard indeed. It is also important to bear in mind that use of any of these parameters alone could lead to erroneous conclusions.

6 Conclusions

The research summarized here was directed at the preparation and characterization of phosphane ligands that would favor the formation of isobutanal in propene hydroformylation. Rh-catalysts prepared from the most thoroughly studied ligands, *o*-alkyl-substituted arylphosphanes, showed promising selectivity for isobutanal, but linear *n*-butanal was still the main product, though only barely. Moreover, the selectivity increased at the cost of activity. Isopropyls in meta position appeared to increase catalyst activity and the initial rate of propene hydroformylation to levels slightly higher than in the case of the reference ligand PPh₃. However, the *m*-isopropyl-substituted phenylphosphanes affected the selectivity in the opposite direction, giving lower i/n ratios than the corresponding *o*-alkyl-substituted phenylphosphanes. *o*-Alkyl substituents near the coordination sphere of rhodium had an important steering effect in olefin hydroformylation but the resulting limited space around the rhodium center reduced the activities of the catalysts.

¹³C{¹H} and ³¹P{¹H} NMR spectra of the *o*-alkyl-substituted phosphane ligands gave parameters, which together with cone angles could be used in search for correlations between properties of ligands and their catalytic behavior. In the hydroformylation of propene with Rh-catalysts modified with closely related *o*-alkyl-substituted phenylphosphanes, correlations were apparent between the catalytical behavior (selectivity to isobutanal and initial rate) and the parameters (cone angle, ³¹P NMR shift and ¹³C NMR shift of C⁷). The selectivity to isobutanal increased as the cone angle and the ¹³C shift of carbon C⁷ increased and decreased as the ³¹P shift increased. However, the initial rate decreased as the cone angle and the ¹³C shift of carbon C⁷ increased, and increased as the ³¹P shift increased. These results suggest the need for additional studies with a larger series of related phosphane ligands. Even now, however, the parameters can roughly predict the catalytical behavior of closely related *o*-alkyl-substituted phenylphosphanes. The several correlations of the different parameters illustrate, as well, that separation of steric and electronic effects of phosphane ligands is difficult.

References

1. Pignolet LH (1983) *Homogeneous Catalysis with Metal Phosphine Complexes*. Plenum Press, New York, p. 7-8, 239.
2. Spessard GO, Miessler GL (1997) *Organometallic Chemistry*. Prentice-Hall, New Jersey, p. 48-137.
3. Leigh GJ, Winterton N (2002) *Modern Coordination Chemistry. The legacy of Joseph Chatt*. The Royal Society of Chemistry, Cambridge, UK.
4. Shriver DF, Atkins PW, Langford CH (1994) *Inorganic Chemistry*. Oxford University Press, p. 715.
5. Quin LD (2000) *A Guide to Organophosphorus Chemistry*, John Wiley & Sons Inc, New York, p. 2, 68-71, 375-376.
6. Xiao S-X, Trogler WC, Ellis DE, Berkovitch-Yellin Z (1983) Nature of the frontier orbitals in phosphine, trimethylphosphine, and trifluorophosphine. *J Am Chem Soc* 105: 7033-7037.
7. Marynick DS (1984) π -Accepting abilities of phosphines in transition-metal complexes. *J Am Chem Soc* 106: 4064-4065.
8. Orpen AG, Connelly NG (1985) Structural evidence for the participation of P-X σ^* orbitals in metal-PX₃ bonding. *J Chem Soc Chem Commun*: 1310-1311.
9. Morris RJ, Girolami GS (1990) On the π -donor ability of early transition metals: evidence that trialkylphosphines can engage in π -back-bonding and X-ray structure of the titanium(II) phenoxide Ti(OPh)₂(dmpe)₂. *Inorg Chem* 29: 4167-4169.
10. Pacchioni G, Bagus PS (1992) Metal-phosphine bonding revisited. σ -Basicity, π -acidity, and the role of phosphorus d orbitals in zerovalent metal-phosphine complexes. *Inorg Chem* 31: 4391-4398.
11. Vogler A, Kunkely H (2002) Excited state properties of transition metal phosphine complexes. *Coord Chem Rev* 230: 243-251.
12. Dias PB, Minas de Pidade ME, Simões JAM (1994) Bonding and energetics of phosphorus(III) ligands in transition metal complexes. *Coord Chem Rev* 135/136: 737-807.
13. Tolman CA (1970) Electron donor-acceptor properties of phosphorus ligands. Substituent additivity. *J Am Chem Soc* 92: 2953-2956.
14. Tolman CA (1970) Phosphorus ligand exchange equilibria on zerovalent nickel. A dominant role for steric effects. *J Am Chem Soc* 92: 2956-2965.
15. Tolman CA, Reutter DW, Seidel WC (1976) A calorimetric study of steric effects in the reactions of phosphorus ligands with Ni(COD)₂. *J Organomet Chem* 117: C30-C33.
16. Tolman CA (1977) Steric effects of phosphorus ligands in organometallic chemistry and homogeneous catalysis. *Chem Rev* 77: 313-348.
17. Brown TL, Lee KJ (1993) Ligand steric properties. *Coord Chem Rev* 128: 89-116.

18. White D, Coville NJ (1994) Quantification of steric effects in organometallic chemistry. *Adv Organomet Chem* 36: 95-158.
19. Casey CP, Whiteker GT (1990) The natural bite angle of chelating diphosphines. *Isr J Chem* 30: 299-304.
20. Streuli CA (1960) Determination of basicity of substituted phosphines by nonaqueous titrimetry. *Anal Chem* 32: 985-987.
21. Streuli CA (1959) Titration characteristics of organic bases in nitromethane. *Anal Chem* 31: 1652-1654.
22. Allman T, Goel RG (1982) The basicity of phosphines. *Can J Chem* 60: 716-722.
23. Grim SO, Yankowsky AW (1977) Phosphorus-31 nuclear magnetic resonance studies on hydrobromides of substituted triarylphosphines and other derivatives. *J Org Chem* 42: 1236-1239.
24. Allen DW, Taylor BF (1982) The chemistry of heteroarylphosphorus compounds. Part 15.1 Phosphorus-31 nuclear magnetic resonance studies of the donor properties of heteroarylphosphines towards selenium and platinum(II). *J Chem Soc, Dalton Trans*: 51-54.
25. Leither W, Bühl M, Fornika R, Six C, Baumann W, Dinjus E, Kessler M, Krüger C, Ruffinška A (1999) ^{103}Rh chemical shifts in complexes bearing chelating bidentate phosphine ligands. *Organometallics* 18: 1196-1206.
26. Weiner MA, Lattman M (1975) Ultraviolet photoelectron spectra of some substituted triarylphosphines. *J Org Chem* 40: 1292-1294.
27. Bancroft GM, Diegnard-Bailey L, Puddephatt R (1986) Spectroscopic study of the effect of methyl and phenyl substituents on the basicity of phosphine ligands in tungsten carbonyl derivatives. *Inorg Chem* 25: 3675-3680.
28. Serron S, Huang J, Nolan SP (1998) Solution thermochemical study of tertiary phosphine ligand substitution reaction in the $\text{Rh}(\text{acac})(\text{CO})(\text{PR}_3)$ system. *Organometallics* 17: 534-539.
29. Huang J, Serron S, Nolan SP (1998) Enthalpies of reaction of $[(p\text{-cymene})\text{OsCl}_2]_2$ with monodentate tertiary phosphine ligands. Importance of steric and electronic ligand factors in an osmium(II) system. *Organometallics* 17: 4004-4008.
30. Haar CM, Nolan SP, Prock A, Giering WP (1998) Synthetic, structural, and solution thermochemical studies in the dimethylbis(phosphine)platinum(II) system. Dichotomy between structural and thermodynamic trends. *Organometallics* 18: 474-479.
31. Suresh CH, Koga N (2002) Quantifying the electronic effect of substituted phosphine ligands via molecular electrostatic potential. *Inorg Chem* 41: 1573-1578.
32. Wilson MR, Liu H, Prock A, Giering WP (1993) Reinvestigation of oxidative addition of MeI , H_2 , and O_2 to $\text{Ir}(\text{CO})(\text{Cl})\text{L}_2$. Quantitative analysis of ligand effects (QALE). *Organometallics* 12: 2044-2050.
33. Wilson MR, Woska DC, Prock A, Giering WP (1993) The quantitative analysis of ligand effects (QALE). The aryl effect. *Organometallics* 12: 1742-1752.
34. Fernandez AL, Reyes C, Prock A, Giering WP (2000) The stereoelectronic parameters of phosphites. The quantitative analysis of ligand effects (QALE). *J Chem Soc, Perkin Trans 2*: 1033-1041.
35. Lau SS, Fanwick PE, Walton RA (2000) The synthesis and characterization of multiply bonded dirhenium(II) alkoxide complexes containing two or three alkoxide ligands, including further studies on complexes of the type $\text{Re}_2\text{Cl}_4(\text{OMe})_2(\text{PAr}_3)_2$ (Ar = aryl). *Inorganica Chimica Acta* 308: 8-16.
36. Howard ST, Foreman JP, Edwards PG (1996) Electronic structure of aryl- and alkylphosphines. *Inorg Chem* 35: 5805-5812.
37. Oswald AA, Hendriksen DE, Kastrup RV, Mozeleski EJ (1992) Electronic effects on the synthesis, structure, reactivity, and selectivity of rhodium hydroformylation catalysts. *Adv Chem Ser* 230: 395-418.
38. Oswald AA, Hendriksen DE, Kastrup RV, Irikura K, Mozeleski EJ, Young DA (1987) Steric effects on the synthesis, structure, reactivity and selectivity of t-phosphine rhodium complex hydroformylation catalysts. *Phosphorus and Sulfur* 30: 237-240.

39. Simpson MC, Cole-Hamilton DJ (1996) Catalytic applications of rhodium complexes containing trialkylphosphines. *Coord Chem Rev* 155: 163-207.
40. Cornils B, Herrmann WA (1996) Applied Homogeneous Catalysis with Organometallic Compounds, VCH, Weinheim, Germany, Vol. 1 and Vol. 2.
41. Van Leeuwen PWNM, Claver C (2000) Rhodium Catalyzed Hydroformylation. Kluwer Academic Publishers, Dordrecht, The Netherlands.
42. Chakrapani H, Liu C, Widenhofer RA (2003) Enantioselective cyclization/hydrosilylation of 1,6-enynes catalyzed by a cationic rhodium bis(phosphine) complex. *Org Lett* 5: 157-159.
43. Goertz W, Kleim W, Vogt D, Englert U, Boele MDK, van der Veen LA, Kamer PCJ, van Leeuwen PWNM (1998) Electronic effects in the nickel-catalysed hydrocyanation of styrene applying chelating phosphorus ligands with large bite angles. *J Chem Soc, Dalton Trans*: 2981-2988.
44. Joó F, Kathó Á (1997) Recent developments in aqueous organometallic chemistry and catalysis. *J Mol Catal A, Chem* 116: 3-26.
45. Trezeciak AM, Ziólkowski JJ (1999) Perspectives of rhodium organometallic catalysis. Fundamental and applied aspects of hydroformylation. *Coord Chem Rev* 190-192: 883-900.
46. Cornils B, Wiebus E (1995) Aqueous catalysts for organic reactions. *Chemtech* 25: 33-38.
47. Chan ASC, Chen CC, Cao R, Lee MR, Peng SM, Lee GH (1997) New rhodium pyridylphosphine complexes and their application in hydrogenation reactions. *Organometallics* 16: 3469-3473.
48. Buhling A, Kamer PCJ, van Leeuwen PWNM (1995) Rhodium catalysed hydroformylation of higher alkenes using amphiphilic ligands. *J Mol Catal A: Chem* 98: 69-80.
49. Buhling A, Kamer PCJ, van Leeuwen PENM, Elgersma JW (1997) Rhodium catalysed hydroformylation of higher alkenes using amphiphilic ligands: part 2. *J Mol Catal A: Chem* 116: 297-308.
50. Breit B, Seiche W (2001) Recent advances on chemo-, regio- and stereoselective hydroformylation. *Synthesis* 1: 1-36.
51. Gladiali S, Bayón JC, Claver C (1995) Recent Advances in Enantioselective Hydroformylation. *Tetrahedron: Asymmetry* 6: 1453-1474.
52. Beller M, Cornils B, Frohning CD, Kohlpaintner CW (1995) Progress in hydroformylation and carbonylation. *J Mol Catal A* 104: 17-85.
53. Palo DR, Erkey C (2000) Effect of ligand modification on rhodium-catalyzed homogeneous hydroformylation in supercritical carbon dioxide. *Organometallics* 19: 81-86.
54. Ancilotti F, Lami M, Marchionna M (1990) Hydroformylation of Z-2-butene with the PtCl₂(cod)/SnCl₂/L catalytic system. Part 3. The effect of the phosphorus ligand L. *J Mol Catal* 63: 15-30.
55. Buhling A, Elgersma JW, Nkrumah S, Kamer PCJ, van Leeuwen PWNM (1996) Novel amphiphilic diphosphines: synthesis, rhodium complexes, use in hydroformylation and rhodium recycling. *J Chem Soc, Dalton Trans*: 2143-2154.
56. Mingos DMP, Müller TE (1995) Complexes of gold(I) with polyaromatic phosphine ligands (1995) *J Organomet Chem* 500: 251-259.
57. Müller TE, Ingold F, Menzer S, Mingos DMP, Williams DJ (1997) Platinum(I) dimers and platinum(0) triangles with polyaromatic phosphine ligands. *J Organomet Chem* 528: 163-178.
58. Müller TE, Green JC, Mingos DMP, McPartlin CM, Whittingham C, Williams DJ, Woodroffe TM (1998) Complexes of gold(I) and platinum(II) with polyaromatic phosphine ligands. *J Organomet Chem* 551: 313-330.
59. Reinius HK, Laitinen RH, Krause AOI, Pursiainen JT (2000) Aspects of regioselective control in the hydroformylation of methyl methacrylate with the *in situ* formed (*o*-thiomethylphenyl)diphenylphosphine rhodium complex. *Stud Surf Sci Catal* 130: 551-556.
60. Culcasi M, Berchadsky Y, Gronchi G, Tordo P (1991) Anodic behavior of crowded triarylphosphines. ESR study of triarylphosphoniumyl radicals, Ar₃P^{•+}. *J Org Chem* 56: 3537-3542.

61. Lobana TS, Paul S, Castineiras A (1997) The chemistry of pyridinethiols and related ligands—VII. Preparation and spectroscopy of mixed-ligand copper(I) complexes: The crystal structure of first mixed-ligand dinuclear [iodo(pyridine-2-thione)(tri-*p*-tolylphosphine)copper(I)]₂ complex. *Polyhedron* 16: 4023-4031.
62. Romain JF, Ribblett JW, Byrn RW, Snyder RD, Storhoff BN, Huffman JC (2000) Synthesis and properties of phenyl phosphines with meta-positioned methyl groups and the X-ray structure of tris(3,5-dimethyl-4-methoxyphenyl)phosphine. *Organometallics* 19: 2047-2050.
63. Barbelis M, Pérez-Prieto J, Herbst K, Lahuerta P (2002) Chiral dirhodium(II) catalysts with ortho-metalated arylphosphine ligands: synthesis and application to the enantioselective cyclopropanation of α -diazo ketones. *Organometallics* 21: 1667-1673.
64. Carey FA, Sundberg RJ (2000) *Advanced Organic Chemistry. Part A: Structure and Mechanisms*. Kluwer Academic/Plenum Publishers, New York, p. 551-567.
65. Davies WC, Mann FG (1944) The stereochemistry of organic derivatives of phosphorus. Part I. The synthesis of acidic and basic dissymmetric tertiary phosphines. The optical resolution of phenyl-*p*-(carboxymethoxy)phenyl-*n*-butylphosphine sulphide. *J Chem Soc*: 276-283.
66. Buchner B, Lockhart LB (1951) An improved method of synthesis of aromatic dichlorophosphines. *J Am Chem Soc* 73: 755-756.
67. Laitinen RH, Heikkinen V, Haukka M, Koskinen AMP, Pursiainen J (2000) 2-Thioanisyl-dichlorophosphine, new starting material for the preparation of multidentate phosphine ligands. Syntheses and characterization of derivatives of 2-anisyl- and 2-thioanisyl-dichlorophosphines. *J Organomet Chem* 598: 235-242.
68. Reinius HK, Laitinen RH, Krause AOI, Pursiainen JT (1999) Hydroformylation of methyl methacrylate with heterodonor phosphinerhodium catalysts prepared *in situ*. *Catal Lett* 60: 65-70.
69. Miller GR, Yankowsky AW, Grim SO (1969) NMR spectra of some CF₃-substituted triphenylphosphines. Evidence for "through-space" P-F spin-spin coupling. *J Chem Phys* 51: 3185-3190.
70. Eapen KC, Tamborski J (1980) The synthesis of tris-(trifluoromethylphenyl)phosphines and phosphine oxides. *J Fluorine Chem* 15: 239-243.
71. Dyer G, Meek DW (1967) Five-coordination. VI. Low-spin cobalt(II) complexes with bidentate ligands. *J Am Chem Soc* 89: 3983-3987.
72. Dyer G, Meek DW (1967) Five-coordination. III. Trigonal-bipyramidal nickel(II) complexes with a phosphorus-selenium tetradentate ligand. *Inorg Chem* 6: 149-153.
73. Wesemann J, Jones PG, Schomburg D, Heuer L, Schmutzler R (1992) Phosphorus derivatives of anthracene and their dimers. *Chem Ber* 125: 2187-2197.
74. Meek DW, Dryer G, Workman Mo (1976) Bi-, tri- and tetradentate phosphorus-sulfur ligands. *Inorg Synth* 16: 168-174.
75. Horner L, Simons G (1983) *Phosphororganische Verbindungen* 101 tertiäre Phosphine mit ortho-alkoxyphenyl-Gruppen. *Synthese und Eigenschaften*. *Phosphorus and Sulphur* 14: 189-209.
76. Jakobsen HJ, Liptaj T, Bundgaard T, Sørensen (1977) Indirect observation of block-siebert shifts in ¹³C-¹H multiple-resonance experiments. *J Magn Reson* 26: 71-79.
77. Mitterhofer F, Schindlbauer H (1967) Über die thermische Stabilität aromatischer tertiärer Phosphine. *Monatsh Chem* 98: 206-213.
78. Schindlbauer H (1965) Umsetzung von Alkalimetallphosphiden mit Salzen aromatischer Sulfonsäuren, 2. Mitt.: Die Reaktion substituierter aromatischer Sulfonate mit Kaliumdiphenylphosphid. *Monatsh Chem* 96: 2051-2057.
79. Kurtev K, Ribola D, Jones RA, Cole-Hamilton DJ, Wilkinson G (1980) Tris(2-pyridyl)-phosphine complexes of ruthenium(II) and rhodium(I). Hydroformylation of hex-1-ene by rhodium complexes. *J Chem Soc, Dalton Trans*: 55-58.
80. Drent E (1991) Preparation of esters of alpha-ethylenically unsaturated alcohols. GB patent 2,240,545.

81. Bowen RJ, Garner AC, Berners-Price SJ, Jenkins ID, Sue RE (1998) Convenient synthetic routes to bidentate and monodentate 2-, 3- and 4-pyridyl phosphines: potentially useful ligands for water-soluble complex catalysts. *J Organomet Chem* 554:181-184.
82. MacDougall JK, Simpson MC, Green MJ, Cole-Hamilton DJ (1996) Direct formation of alcohols by hydrocarbonylation of alkenes under mild conditions using rhodium trialkylphosphine catalysts. *J Chem Soc Dalton Trans*: 1161-1172.
83. Huang Y, Haewon LU, Gilson DFR, Butler IS (1997) Phosphorus-31 chemical shift anisotropies in solid, octahedral chromium(0) triphenylphosphine derivatives. *Inorg Chem* 26: 435-438.
84. Meintjies E, Singleton E, Schmutzler R, Sell M (1985) Complexes of rhodium(I) and iridium(I) with mixed phosphorus-oxygen and phosphorus-nitrogen ligands. *S Afr J Chem* 38: 115-120.
85. Laitinen RH, Riihimäki H, Haukka M, Jääskeläinen S, Pakkanen TA, Pursiainen J (1999) Syntheses and characterization of new tertiary phosphane ligands prepared from *p*-anisyl- and *p*-thioanisyl-dichlorophosphanes. *Eur J Inorg Chem*: 1253-1258.
86. Hirsivaara L, Haukka M, Jääskeläinen S, Laitinen RH, Niskanen E, Pakkanen TA, Pursiainen J (1999) Organometallic derivatives of multidentate phosphines [*o*-(methylthio)phenyl]-diphenylphosphine and bis(*o*-(methylthio)phenyl)phenylphosphine: preparation and characterization of group 6 metal carbonyl derivatives. *J Organomet Chem* 579: 45-52.
87. Abdur-Rashid K, Fong TP, Greaves B, Gusev DG, Hinman JG, Landau SE, Lough AJ, Morris RH (2000) An acidity scale for phosphorus-containing compounds including metal hydrides and dihydrogen complexes in THF: toward the unification of acidity scales. *J Am Chem Soc* 122: 9155-9171.
88. Potyen MC, Rothwell IP (1995) Regio- and stereo-selectivity in the hydrogenation of aryl phosphines by niobium aryloxide compounds. *J Chem Soc, Chem Commun*: 849-851.
89. Williams DH, Fleming I (1995) *Spectroscopic Methods in Organic Chemistry*. McGraw-Hill Book Company Europe, London, p. 151-160.
90. McFarlane W (1968) Chemical shift and coupling constant nonequivalence of isopropyl methyl protons in a tertiary phosphine. *Chem Communications*: 229-230.
91. Schraml J, Čapka M, Blechta V (1992) ³¹P and ¹³C NMR spectra of cyclohexylphenylphosphines, tricyclohexylphosphine and triphenylphosphine. *Magn Reson Chem* 30: 544-547.
92. Schraml J, Blechta V, Krahé E (1992) Long-range 2d inadequate in structure determination. *Collect Czech Chem Commun* 57: 2005-2011.
93. Kunze U, Jawad H (1986) Penta- und Tetracarbonylmetall-Komplexe des Chroms, Molybdäns und Wolframs mit sekundären und tertiären Phosphinothioformamid-Liganden. *Z Anorg Allg Chem* 532: 107-117.
94. Garrou P (1981) Δ_R Ring contributions to ³¹P NMR parameters of transition-metal-phosphorus chelate complexes. *Chem Rev* 81: 229-266.
95. Moser WR, Papile CJ, Brannon DA, Duwell RA, Weininger SJ (1987) The mechanism of phosphine-modified rhodium-catalyzed hydroformylation studied by CIR-FTIR. *J Mol Catal* 41: 271-292.
96. Unruh JD, Christenson JR (1982) A study of the mechanism of rhodium/phosphine-catalyzed hydroformylation: use of 1,1'-bis(diarylphosphino)ferrocene ligands. *J Mol Catal* 14: 19-34.
97. Van Leeuwen PWNM, Roobeek CF (1983) Hydroformylation of less reactive olefins with modified rhodium catalysts. *J Organomet Chem* 258: 343-350.
98. Van Rooy A, Orij EN, Kamer PCJ, van den Aardweg F, van Leeuwen PWNM (1991) Hydroformylation of oct-1-ene with extremely high rates using rhodium catalysts containing bulky phosphites. *J Chem Soc, Chem Commun*: 1096-1097.
99. Van Rooy, Orij EN, Kamer PCJ, van Leeuwen PWNM (1995) Hydroformylation with a rhodium/bulky phosphite modified catalyst. Catalyst comparison for oct-1-ene, cyclohexene, styrene. *Organometallics* 14: 34-43.
100. Jongsma T, Challa G, van Leeuwen PWNM (1991) A mechanistic study of rhodium tri(*o*-*t*-butylphenyl)phosphite complexes as hydroformylation catalysts. *J Organomet Chem* 421: 121-128.

101. Oswald AA, Merola JS, Reisch JC, Kastrup RV (1984) High temperature hydroformylation. US patent, WO 84/03697.
102. Poelsma SN, Maitlis PM (1993) Rhodium catalysed hydroformylation using slim phosphate ligands to improve selectivity. *J Organomet Chem* 451: C15-C17.
103. Bianchini C, Frediani P, Meli A, Peruzzini M, Vizza F (1997) 1-Hexene hydroformylation with rhodium(I) triphosphane complex $[\text{Rh}(\text{CO})\{\text{PhP}(\text{CH}_2\text{CH}_2\text{PPh}_2)_2\}]\text{PF}_6^-$: an in situ study using high-pressure NMR spectroscopy. *Chem Ber/Recueil* 130: 1633-1641.
104. Beller M, Zimmermann B, Geissler H (1999) Dual catalytic systems for consecutive isomerization–hydroformylation reactions. *Chem Eur J* 5: 1301-1305.
105. Trzeciak AM, Szterenberga L, Wolszczak E, Ziolkowski JJ (1995) Effect of ligand donor–acceptor properties on selectivity of catalytic olefin isomerization reaction. *J Mol Catal A, Chem* 99: 23-28.
106. Salvini A, Piacenti F, Frediani P, Devescovi A, Caporali M (2001) Isomerization of olefins by phosphine-substituted ruthenium complexes and influence of an ‘additional gas’ on the reaction rate. *J Organomet Chem* 625: 255-267.
107. Suomalainen P, Jääskeläinen S, Haukka M, Laitinen RH, Pursiainen J, Pakkanen TA (2000) Structural and theoretical studies of *ortho*-substituted triphenylphosphane ligands and their rhodium(I) complexes. *Eur J Inorg Chem*: 2607-2613.
108. Friebolin H (1998) *Basic One- and Two-Dimensional NMR Spectroscopy*. Wiley-VCH, Weinheim, Germany, p. 49-50.